

AD-A040 935

MASSACHUSETTS INST OF TECH CAMBRIDGE DEPT OF METEOROLOGY F/G 4/2  
A STUDY OF FORECAST ERRORS IN AN OPERATIONAL MODEL FOR PREDICTI--ETC(U)  
DEC 76 E SANDERS, N J GORDON AFGL-TR-77-0079 F19628-75-C-0059 NL

UNCLASSIFIED

SCIENTIFIC-2

AFGL-TR-77-0079

NL

AD  
A040 935



END

DATE  
FILMED  
7-77

AD A 040935

AFGL-TR-77-0079

A STUDY OF FORECAST ERRORS IN AN OPERATIONAL MODEL  
FOR PREDICTING PATHS OF TROPICAL STORMS.

Frederick Sanders  
Norma J. Gordon

Department of Meteorology  
Massachusetts Institute of Technology  
Cambridge, Massachusetts 02139

December 1976

Scientific Report No. 2

Approved for public release; distribution unlimited

AD No. \_\_\_\_\_  
DDC FILE COPY

AIR FORCE CAMBRIDGE RESEARCH LABORATORIES  
AIR FORCE SYSTEMS COMMAND  
UNITED STATES AIR FORCE  
HANSCOM AFB, MASSACHUSETTS 01731



Unclassified

SECURITY CLASSIFICATION OF THIS PAGE (When Data Entered)

REPORT DOCUMENTATION PAGE		READ INSTRUCTIONS BEFORE COMPLETING FORM
1. REPORT NUMBER AFGL-TR-77-0079	2. GOVT ACCESSION NO.	3. RECIPIENT'S CATALOG NUMBER
4. TITLE (and Subtitle) A STUDY OF FORECAST ERRORS IN AN OPERATIONAL MODEL FOR PREDICTING PATHS OF TROPICAL STORMS	5. TYPE OF REPORT & PERIOD COVERED Scientific Report No. 2	
7. AUTHOR(s) Frederick Sanders Norma J. Gordon	6. PERFORMING ORG. REPORT NUMBER	
9. PERFORMING ORGANIZATION NAME AND ADDRESS Department of Meteorology Massachusetts Institute of Technology Cambridge, Massachusetts 02139	8. CONTRACT OR GRANT NUMBER(s) F19628-75-C-0059	
11. CONTROLLING OFFICE NAME AND ADDRESS Air Force Geophysics Laboratory Hanscom AFB, Massachusetts 01731 Monitor/Thomas Keegan/LYS	10. PROGRAM ELEMENT, PROJECT, TASK AREA & WORK UNIT NUMBERS 62101F 86281201	
14. MONITORING AGENCY NAME & ADDRESS (if different from Controlling Office) Scientific-2	12. REPORT DATE December 1976	
	13. NUMBER OF PAGES	
	15. SECURITY CLASS. (of this report) Unclassified	
	15a. DECLASSIFICATION/DOWNGRADING SCHEDULE	
16. DISTRIBUTION STATEMENT (of this Report) Approved for public release; distribution unlimited.		
17. DISTRIBUTION STATEMENT (of the abstract entered in Block 20, if different from Report) 8628 12		
18. SUPPLEMENTARY NOTES		
19. KEY WORDS (Continue on reverse side if necessary and identify by block number) Tropical Storms Dynamical prediction Satellite observations		
20. ABSTRACT (Continue on reverse side if necessary and identify by block number) We have studied the SANBAR forecasts made operationally at the National Hurricane Center during the 1975 hurricane season. The forecast model is a barotropic one designed explicitly for predicting the tracks of tropical storms, and is based on direct analysis of the wind field averaged through the depth of the troposphere. Our concern is primarily to assess the possible impact of increased use of satellite observations in the initial analysis, but we are also interested in identifying the various sources of forecasts error, including		

220023

Handwritten signature/initials

(but not limited to) faulty initial analysis. ←

Our findings are that:

1. A more accurate initial position and track approaching the accuracy of the post-season "best-track" analysis, will produce a substantial increase in accuracy of the position forecasts at ranges of 24 hours and probably at 48 hours.
2. The use of satellite-derived heights may provide useful information for prediction of storms initially poleward of, say, 30°N.
3. The current method of analyzing the initial stream-function field in the area influenced by the storm circulation results in a loss of useful observations (mainly satellite-derived wind estimates) in the outer fringes.
4. Fixed values of stream-function and absolute vorticity on the boundaries of the current SANBAR forecast grid are producing serious errors beyond 24 hours range in some storms in, or recurving into, the westerlies of middle latitudes.
5. Some storm tracks respond to baroclinic effects in the large-scale features of the surrounding region. In some additional instances the storm track may be directly influenced by asymmetric baroclinic effects in the storm structure itself.



# TABLE OF CONTENTS

	Page
List of Tables.....	4
List of Figures.....	5
Acknowledgements.....	7
Introduction.....	8
Use of Best Track Positions and Displacement Vectors.....	11
Identification of the Predicted Storm Center.....	20
SANBAR Analysis in Oceanic Regions.....	25
Diagnosis of Error in some 1975 Forecasts.....	32
Amy, July 3, 0000GMT.....	32
Faye, September 26, 0000GMT.....	39
Gladys, September 30, 0000GMT.....	48
Conclusions.....	53
References.....	56

ACCESSION FOR	
RTIS	White Section <input checked="" type="checkbox"/>
DDC	Buff Section <input type="checkbox"/>
UNANNOUNCED	<input type="checkbox"/>
JUSTIFICATION.....	
BY.....	
DISTRIBUTION/AVAILABILITY CODES	
.....	
.....	

A

DDC  
**RECEIVED**  
 JUN 27 1977  
**RECEIVED**  
 D

## TABLES

	<u>Page</u>
Table 1. Displacement errors (nautical miles) for 1975 guidance forecasts.....	9
Table 2. Operational and best-track initial positions and displacement vectors.....	12
Table 3. Mean position errors (nautical miles ) for operational forecasts.....	15
Table 4. Mean position errors (nautical miles) for SANBAR reruns.....	16
Table 5. Mean magnitudes of speed and direction errors.....	19
Table 6. Algebraic means of speed and direction errors.....	21
Table 7. Mean position errors (nautical miles) for SANBAR reruns based on vorticity maximum alone.....	23
Table 8. Mean algebraic errors of original rerun forecasts and of reruns based on vorticity maximum alone.....	24
Table 9. Regression equations for zonal and meridional components (knots) of mean tropospheric wind, based on rawinsonde observations at 850 mb and 200 mb.....	29
Table 10. List of cases for revised forecasts.....	31
Table 11. Position errors (nautical miles) in SANBAR forecasts for Faye, September 26, 0000GMT.....	39
Table 12. Position errors (nautical miles) in SANBAR forecasts for Gladys, September 30, 0000GMT...	48

# FIGURES

	<u>Page</u>
Figure 1. Best tracks of 1975 storms.....	10
Figure 2. Sketch illustrating speed and direction errors....	18
Figure 3. Sketches of correction for "nominal position" forecasts and for "vorticity maximum" forecasts, with actual values of mean discrepancies given in nautical miles.....	26
Figure 4. Map of SANBAR grid with bogus points and sample of computational grid.....	27
Figure 5. Tracks of Amy, July 3, 0000GMT. Dashed lines indicate observed track; solid lines, operational track; and dotted lines, best-track rerun. Dots show forecast positions, labelled with the appropriate number of hours after initial time. Corresponding observed positions are shown by hurricane symbols with open centers, indicating tropical storm strength.....	33
Figure 6. Initial analysis of large scale flow pattern, July 3, 0000GMT. Solid lines are isopleths of stream function, at intervals of $300 \times 10^4 \text{ m}^2 \text{ s}^{-1}$ from the operational SANBAR analysis. Dashed lines are subjectively analyzed 500-mb contours at intervals of 6 dm. Triangles indicate 500-mb heights obtained from satellite data; circles, from rawinsonde observations.....	35
Figure 7. Data bases for oceanic analysis, July 3, 0000GMT: a) ATOLL, b) 200-mb. Positions of bogus points are shown by circled x's. Radius of influence is shown by the dashed circle. Dashed arrows indicate data not in NHC collection.....	36
Figure 8. Wind fields from a) the subjective 500-mb geostrophic analysis and b) subjectively-smoothed SANBAR initial analysis. Dotted lines indicate isotachs at 10-kt intervals. Other notation the same as Figure 6.....	38
Figure 9. Tracks of Faye, September 26, 0000GMT. Hurricane symbols with closed centers indicate storm of hurricane strength. Other notation the same as Figure 5.....	40

## FIGURES

	<u>Page</u>
Figure 10. Initial SANBAR operational flow pattern, September 26, 0000GMT. Solid arrows indicate winds derived from stream-function pattern. Dashed arrows indicate winds estimated from ATOLL and 200-mb data bases.....	42
Figure 11. Data bases for oceanic analysis, September 26, 0000GMT: a) ATOLL, b) 200-mb. Notation the same as Figure 7.....	43
Figure 12. Large scale initial flow pattern (solid lines) and 48-hour stream-function changes: a) observed; b) predicted by SANBAR. Dashed lines indicate stream-function rises; dotted lines, stream-function falls.....	45
Figure 13. NMC prognostic charts: a) 36-hour barotropic forecast valid at 0000GMT, September 27; b) 24-hour PE forecast valid at 0000GMT, September 27; and c) 72-hour PE forecast valid at 0000GMT, September 29.....	47
Figure 14. Tracks of Gladys, September 30, 0000GMT. Notation the same as Figures 5 and 9.....	49
Figure 15. Data bases for oceanic analysis, September 30, 0000GMT: a) ATOLL; b) 200-mb. Notation the same as Figure 7.....	50
Figure 16. Large scale initial flow pattern and 48-hour stream-function changes: a) observed; b) predicted by SANBAR. Notation the same as Figure 12.....	52
Figure 17. NMC prognostic charts: a) 36-hour barotropic forecast valid at 1200GMT, October 1; and b) 36-hour PE forecast valid at 1200GMT, October 1.....	54

### ACKNOWLEDGEMENTS

The authors are grateful to Patricia Tayntor, of MIT, for help in plotting and analysis of data, to the National Hurricane Center (especially to Mark Zimmer), for vital cooperation in the SANBAR reruns, to the National Center for Atmospheric Research (especially to Paul Mulder and Roy Jenner) and to NHC, for providing critical data. We are also grateful to Isabelle Kole for preparation of figures and the manuscript.



## INTRODUCTION

The goal of this study is to establish the value of satellite observations for the prediction of tropical cyclones. We are especially concerned with observations which can be derived with ease from the McIDAS system (U. of Wisconsin, 1973) at the Air Force Geophysics Laboratory (AFGL). Moreover, we are particularly concerned with prediction of the cyclone tracks by SANBAR, (Sanders et al. 1975), a barotropic dynamical model applied to the large-scale flow pattern surrounding the storm, averaged through the depth of the tropical troposphere. This model is used operationally at the National Hurricane Center (NHC).

Because of lack of adequate data within the area influenced by the storm, the analysis within this region is modeled on the basis of the estimated size, intensity, and current displacement vector of the storm, as described by Sanders et al. (1975). Elsewhere the analysis is based on winds observed by rawinsondes, by aircraft, and by ships; and (recently) on wind estimates based on cloud-motion vectors derived from geosynchronous satellites.

Our work has focused on improving the accuracy of the SANBAR forecasts through more accurate determination of the position and track of the storm, and through improvement of the large-scale analysis by more extensive use of the satellite wind estimates. In this report, we discuss the first of these efforts in detail, and examine intensively some particularly poor operational forecasts to determine the cause of the errors and to estimate the likelihood of improvement by increased use of the satellite data. All cases were taken from the 1975 hurricane season in the Atlantic Ocean, the Caribbean Sea, and the Gulf of Mexico. The tracks of these storms, determined by careful analysis after the fact (the "best tracks"), are shown in Fig. 1. The real-time performance of SANBAR, of several other guidance forecasts, and of the ultimate "official" prediction issued by NHC, is shown in Table 1. The various other guidance forecasts are discussed by Newmann et al. (1972), Newmann and Hope (1973), and Newmann and Lawrence (1975).

TABLE 1. Displacement errors (nautical miles) for 1975 guidance forecasts.

	<u>12 hour</u>	<u>24 hour</u>	<u>36 hour</u>	<u>48 hour</u>	<u>72 hour</u>
Official	61	126	---	282	395
NHC67	56	134	---	355	459
NHC72	61	133	---	330	401
CLIFER	60	132	---	273	316
NHC73	52	116	---	276	415
SANBAR	65	127	---	268	356
Number of cases	54	45	0	32	26

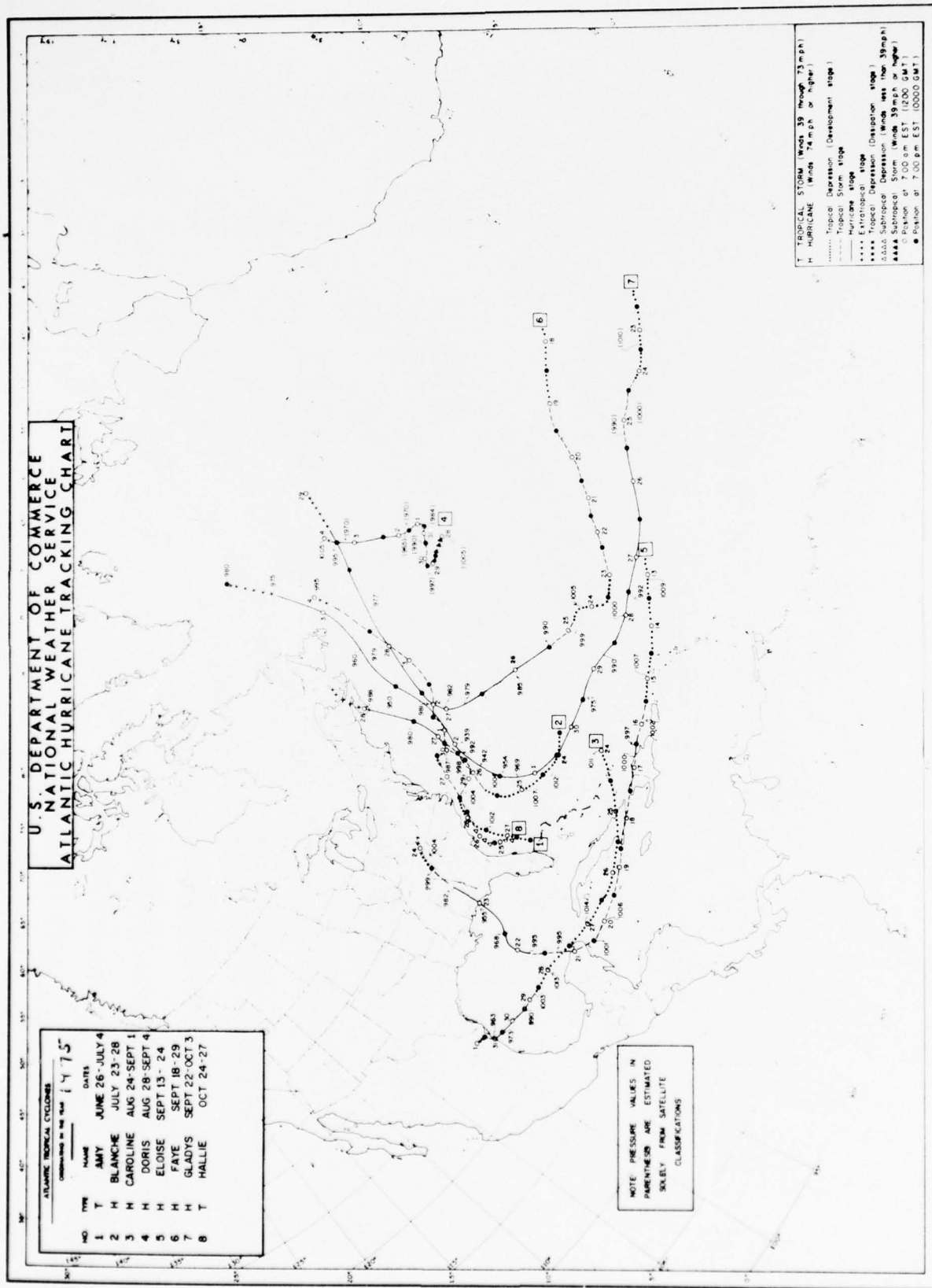


Figure 1. Best tracks of 1975 storms

## USE OF BEST TRACK POSITIONS AND DISPLACEMENT VECTORS

The McIDAS system with its superior navigation offers the possibility of more accurate tracking of a tropical storm up to the initial time of the forecast. This determination could be based on application of the correlation technique (U. of Wisconsin, 1973) either to the storm cloud system as a whole, or, preferably, to the eye if it is discernible. To simulate the best of all possible worlds, we have taken the best-track information for 74 of the 78 cases in which operational SANBAR forecasts were made in 1975.<sup>1</sup> These forecasts were rerun by NHC with the operational data base but with the best-track initial positions and displacement vectors instead of the operational ones. The operational and best-track values are given for each case in Table 2. The best-track vector was obtained from the 6-hour displacement immediately prior to initial time, to simulate the real-time situation.

Position errors for the operational forecasts and for the reruns are summarized in Tables 3 and 4, respectively. Verification in both instances was taken from best-track positions. The number of verifications decreased monotonically with forecast range as increasing numbers of tracks passed inland or eastward out of the range of NHC forecast responsibility. In a few instances the storm weakened within the NHC area so as to obviate the necessity of tracking. It is unlikely that the accuracy of the best-track information could even be achieved in real time, if only because the position at a given time is determined by observed fixes after, as well as before, that time. In real time we will be hard put to know whether the most recent change in track represents a significant change in the displacement rate of the storm, or merely a short-period excursion. Only analysis after the fact can effect that determination. Therefore, the results in Table 4 represent a limit of optimism in this respect.

Subject to the above qualifications, the results show a substantial im-

---

1. The four remaining forecasts could not be rerun for a variety of reasons unrelated to the accuracy of the operational predictions.



TABLE 2. Operational and best-track initial positions and displacement vectors.

Storm	Mo/day	Time(GMT)	OPERATIONAL			BEST-TRACK		
			Lat( $^{\circ}$ N)	Long( $^{\circ}$ W)	Dir( $^{\circ}$ )/spd(kts)	Lat( $^{\circ}$ N)	Long( $^{\circ}$ W)	Dir( $^{\circ}$ )/spd(kts)
Amy	06/30	0000	34.2	71.1	055/10	34.3	71.6	065/12
	06/30	1200	36.0	70.5	030/06	35.9	70.5	035/03
	07/01	0000	36.0	70.0	090/03	36.2	69.8	090/04
	07/01	1200	36.3	68.2	085/10	36.2	68.3	090/08
Blanche	07/02	0000	37.4	66.6	045/10	37.4	66.7	030/09
	07/03	1200	39.5	59.5	045/18	39.3	59.6	050/17
	07/04	0000	42.5	54.8	050/30	42.5	54.8	050/32
	07/26	1200	33.5	73.5	035/15	33.4	73.5	035/14
	07/27	0000	34.9	70.8	055/13	35.0	71.0	050/13
	07/27	1200	36.5	68.5	055/12	36.9	69.0	040/13
	07/28	0000	39.1	67.3	022/13	39.3	67.2	020/16
	08/29	1200	23.2	93.2	284/08	23.2	93.2	270/06
Caroline	08/30	0000	23.3	94.0	000/00	23.3	94.2	280/06
	08/30	1200	23.7	95.8	280/07	23.7	95.6	295/05
	08/31	0000	24.1	97.0	280/04	24.0	97.0	280/05
	08/31	1200	24.3	97.9	285/05	24.3	97.8	285/04
Doris	08/30	1200	25.3	48.1	090/03	35.3	48.0	090/05
	08/31	0000	35.0	45.9	095/08	34.9	45.2	095/05
	09/01	0000	34.3	44.5	115/05	34.5	44.6	090/03
	09/01	1200	34.8	44.0	075/01	34.9	44.0	020/06
Eloise	09/02	0000	35.8	44.1	350/04	35.8	44.4	315/04
	09/02	1200	37.0	44.3	360/06	37.0	44.3	010/07
	09/03	0000	38.5	43.8	010/06	38.4	43.8	025/08
	09/03	1200	40.5	43.2	030/10	41.1	43.0	045/08
	09/04	0000	42.8	42.0	023/10	42.8	42.0	030/08
	09/16	1200	19.3	67.6	275/11	19.4	67.5	280/08
	09/17	0000	19.6	68.9	280/07	19.6	69.2	280/08
	09/17	1200	19.7	70.7	275/08	19.7	71.2	270/10
	09/18	0000	20.1	73.2	275/10	19.9	73.3	275/11
	09/18	1200	20.3	76.1	270/11	19.9	75.7	270/10



TABLE 2. Operational and best-track initial positions and displacement vectors.  
(continued)

Storm	Mo/day	Time(GMT)	OPERATIONAL			BEST-TRACK		
			Lat( $^{\circ}$ N)	Long( $^{\circ}$ W)	Dir( $^{\circ}$ )/spd(kts)	Lat( $^{\circ}$ N)	Long( $^{\circ}$ W)	Dir( $^{\circ}$ )/spd(kts)
Eloise	09/19	0000	19.7	78.3	270/10	20.0	78.2	270/12
	09/19	1200	19.8	80.1	275/12	19.9	79.8	270/06
	09/20	0000	20.5	82.5	280/13	19.8	82.2	270/12
	09/20	1200	20.5	84.5	270/10	19.9	84.6	280/10
	09/21	0000	20.5	86.5	270/10	20.2	86.4	280/10
	09/21	1200	21.4	87.6	290/07	21.4	87.8	325/08
	09/22	0000	23.5	89.0	335/08	23.6	88.9	345/12
	09/22	1200	25.9	89.5	350/12	25.8	89.5	355/10
	09/23	0000	27.4	88.7	055/09	27.3	88.5	050/11
	09/23	1200	30.3	86.4	030/22	30.2	86.3	025/19
Faye	09/20	0000	20.0	41.8	285/12	20.5	41.3	275/10
	09/20	1200	20.3	44.5	280/13	20.3	44.0	260/13
	09/21	0000	20.2	46.8	275/13	20.3	46.2	270/08
	09/21	1200	20.4	48.2	275/11	20.3	47.8	270/07
	09/22	0000	20.5	48.9	275/05	20.5	49.3	275/07
	09/22	1200	20.5	50.5	270/06	20.4	50.8	270/07
	09/23	0000	20.5	52.0	270/07	20.4	52.2	270/07
	09/25	1200	24.9	59.1	310/09	24.8	58.8	315/08
	09/26	0000	26.5	60.4	315/11	26.5	60.0	330/11
	09/26	1200	29.5	62.2	325/18	29.6	62.0	330/19
Gladys	09/27	0000	32.7	64.3	330/18	32.7	64.2	330/18
	09/27	1200	36.1	65.9	325/20	36.1	65.7	345/17
	09/28	0000	38.6	63.5	045/18	38.4	63.7	045/14
	09/28	1200	41.1	57.0	070/30	41.0	57.1	065/30
	09/25	0000	14.2	41.0	310/07	14.2	41.0	315/10
	09/25	1200	15.3	43.1	300/12	15.4	43.0	305/12
	09/26	0000	16.3	45.0	290/11	16.2	45.0	290/10
	09/26	1200	16.6	47.6	280/12	16.6	47.7	275/16

TABLE 2. Operational and best-track initial positions and displacement vectors.  
(continued)

Storm	Mo/day	Time (GMT)	OPERATIONAL			BEST-TRACK		
			Lat(°N)	Long(°W)	Dir(°)/spd(kts)	Lat(°N)	Long(°W)	Dir(°)/spd(kts)
Gladys	09/27	0000	17.2	50.7	280/15	17.1	50.7	285/15
	09/27	1200	17.8	53.7	275/15	18.2	53.7	295/15
	09/28	0000	19.6	56.3	300/15	19.4	56.4	295/13
	09/28	1200	19.7	58.3	270/10	19.8	58.2	295/08
	09/29	0000	21.0	60.5	300/10	21.2	60.3	315/13
	09/29	1200	23.0	62.6	305/15	23.0	62.6	310/14
	09/30	0000	24.1	65.1	295/14	24.1	65.2	295/14
	09/30	1200	25.2	67.9	290/13	25.1	67.9	295/13
	10/01	0000	25.8	70.4	270/13	26.1	70.6	295/13
	10/01	1200	28.0	72.2	340/12	27.9	72.4	330/12
	10/02	0000	30.9	72.9	334/20	31.0	73.0	360/17
	10/02	1200	35.0	70.0	045/30	35.3	69.8	040/31
	10/03	0000	40.3	62.7	055/40	40.8	62.6	050/44
Hallie	10/27	0000	33.7	77.0	045/14	33.5	77.5	045/15
	10/27	1200	35.6	72.5	060/25	35.7	73.8	045/18

TABLE 3. Mean position errors (nautical miles) for operational forecasts.

	<u>00 hr</u>	<u>12 hr</u>	<u>24 hr</u>	<u>36 hr</u>	<u>48 hr</u>	<u>72 hr</u>
Amy	8 (7)	72 (6)	107 (5)	117 (5)	197 (5)	338 (3)
Blanche	16 (4)	53 (3)	101 (2)	135 (1)	--	--
Caroline	7 (5)	33 (4)	73 (3)	116 (2)	152 (1)	--
Doris	11 (10)	72 (9)	104 (8)	174 (7)	240 (6)	369 (4)
Eloise	18 (15)	60 (14)	95 (13)	134 (12)	198 (11)	283 (9)
Faye	19 (14)	73 (13)	151 (11)	218 (9)	268 (7)	483 (5)
Gladys	11 (17)	76 (17)	144 (16)	233 (15)	347 (14)	459 (12)
Hallie	46* (2)	65 (1)	---	---	---	---
Mean	15 (74)	67 (67)	121 (58)	181 (51)	261 (44)	393 (33)

\* Significant at 10% level

() Number in sample

TABLE 4. Mean position errors (nautical miles) for SANBAR) reruns.

	<u>00hr</u>	<u>12hr</u>	<u>24hr</u>	<u>36hr</u>	<u>48hr</u>	<u>72hr</u>	<u>Total</u> *
Amy	0 (7) [7]	63 (6) [3]	111 (5) [3]	155 (5) [2]	237 (5) [1]	400 (3) [1]	(24) [10]
Bianche	0 (4) [4]	27 (3) [3]	72 (2) [2]	137 (1) [0]	--	--	(6) [5]
Caroline	0 (5) [5]	24 (4) [2]	42 (3) [2]	79 (2) [1]	220 (1) [0]	--	(10) [5]
Doris	0 (10) [10]	42 (9) [7]	74 (8) [6]	112 (7) [6]	171 (6) [5]	302 (4) [4]	(34) [28]
Eloise	0 (15) [15]	41 (14) [9]	68 (13) [10]	105 (12) [7]	179 (11) [6]	310 (9) [5]	(59) [37]
Faye	0 (14) [14]	67 (13) [10]	136 (11) [6]	181 (9) [6]	195 (7) [6]	411 (5) [4]	(45) [32]
Gladys	0 (17) [17]	52 (17) [10]	122 (16) [10]	201 (15) [9]	293 (14) [8]	430 (12) [6]	(74) [43]
Hallie	0 (2) [2]	88 (1) [0]	--	--	--	--	(1) [0]
Mean	0 (74) [74]	50 (67) [44]	99 (58) [39]	152 (51) [31]	224 (44) [26]	376 (33) [20]	(253) [160]

Change from operational forecasts

-15      -17      -22      -29      -37      -17

\* Total excluding 00hr

() Number in sample

[ ] Number in sample which had position errors equal to or less than those of operational forecasts.

provement at all ranges. From previous experience we believe that the benefit due to correction of the initial position alone would be a maximum at the initial time and would have largely vanished 48 hours later. Since we find here the greatest improvement in the range from 36 to 48 hours, it appears that the corrected displacement vector, which immediately improves the stream-function analysis in the region influenced by the storm at the initial time, has also a surprisingly beneficial large-scale effect at later times. By 72 hours, however, the improvement is decreasing rapidly.

We note that the mean errors for any forecast range for any individual storm differ only insignificantly from the mean over all storms. That is, none of the 1975 storms were exceptionally difficult (or easy) to predict. This uniformity is probably due to the lack of any notably eccentric tracks during this year, as can be seen by inspection of Fig. 1. In the event of loops, cusps, halts, and sudden starts, it is likely that the best-track information would have differed from the operational data more widely than shown in Table 2. It is thus probable that the improvement in forecast accuracy would be greater. In this respect, then, the improvement shown in Table 4 may understate the potential of the best-track information.

Two aspects of the displacement error vectors were examined, for both the operational and the rerun forecasts. The first of these was simply the speed error, expressed in nautical miles per 24 hours. The second was a "direction error", the perpendicular distance from the forecast position to the observed displacement vector. The definitions of these errors is illustrated by the sketch in Fig. 2. This was done separately for the first and for the second 24-hour periods of each forecast. Results are summarized for mean magnitudes in Table 5 and for algebraic means in Table 6. In the latter, a negative value means too slow a forecast speed, or a forecast position to the left of the observed track, as shown in Fig. 2.

In Table 5 we see that speed errors and direction errors are of comparable magnitude, that both grow substantially from the first to the second 24-hour period of the forecast, and that both types are reduced slightly for both periods in the rerun forecasts. The statistical significance of the improve-



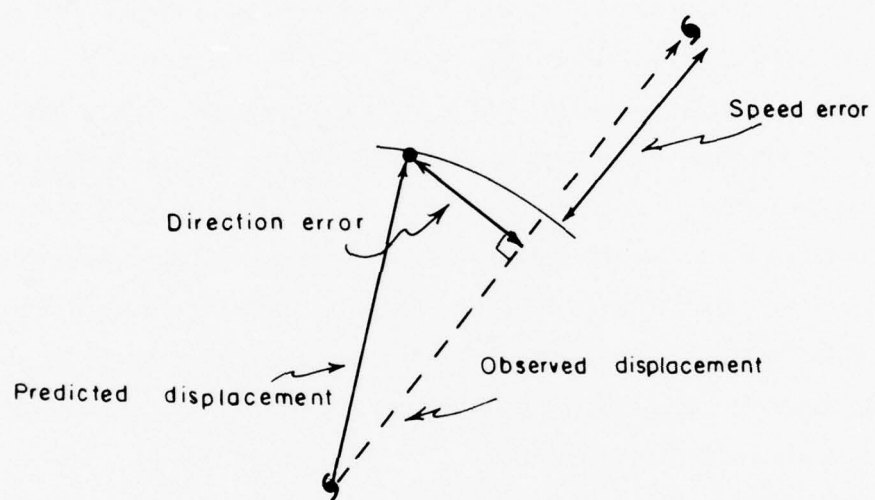


Figure 2 Sketch illustrating speed and direction errors.

TABLE 5. Mean magnitudes of speed and direction errors.

	SPEED ERRORS (nm)				DIRECTION ERRORS (nm)			
	Operational		Reruns		Operational		Reruns	
	00-24hr	24-48hr	00-24hr	24-48hr	00-24hr	24-48hr	00-24hr	24-48hr
Storm								
Amy	34 (5)	96 (5)	72 (5)	144 (5)	93 (5)	74 (5)	81 (5)	66 (5)
Blanche	48 (2)	—	36 (2)	—	54 (2)	—	95 (2)	—
Caroline	55 (3)	72 (1)	0 (3)	72 (1)	18 (3)	74 (1)	53 (3)	139 (1)
Doris	60 (8)	60 (6)	34 (8)	55 (6)	47 (8)	75 (6)	44 (8)	66 (6)
Eloise	46 (13)	41 (11)	38 (13)	19 (11)	70 (13)	101 (11)	43 (13)	96 (11)
Faye	120 (11)	137 (7)	108 (11)	122 (7)	67 (11)	80 (7)	58 (11)	71 (7)
Gladys	98 (16)	166 (14)	94 (14)	170 (14)	82 (16)	107 (14)	77 (16)	80 (14)
Mean	77 (58)	106 (44)	67 (58)	103 (44)	68 (58)	92 (44)	61 (58)	80 (44)

( ) Number in sample

ment in the overall means is not large<sup>1</sup>, but inspection of Table 5 shows that improvement occurred for the individual storm means in about three-quarters of the instances.

In Table 6, some interesting biases appear. The forecast speeds are slow and the displacements are to the left of the observed tracks. Surprisingly, the biases are not reduced in the rerun predictions based on best-track information. Reference to Fig. 1 shows that the 1975 storms tended strongly to move along clockwise-curved tracks (i.e. to recurve) and accelerate during the period when forecasts were made. This tendency was especially pronounced for Eloise, Faye, and Gladys, for which the majority of predictions were made. (In 31 of the 74 cases the initial position was north of  $30^{\circ}\text{N}$ .) Evidently the forecast tracks did not show these characteristics to a sufficient degree, presumably because of a failure in the forecast of the large-scale circulation pattern. The relative success of the operational forecasts in these respects may have been due to a subjective anticipation of this behavior on the part of the hurricane forecasters who provided the operational initial track directions and speeds. We do not believe that this result would be found in a sample of forecasts in which more of the actual tracks were irregular.

#### IDENTIFICATION OF THE PREDICTED STORM CENTER

The nominal position of the storm center in the SANBAR forecast has been taken as the mean of the positions of the absolute vorticity maximum and the stream-function minimum, when both were present. If the latter vanishes, as it often does due to truncation error or strengthening of the large-scale flow in the vicinity of the storm, then the position of the storm is identified with that of the vorticity maximum. In this case, the forecast track displays a spurious jog to the right. Rarely, the forecast vorticity

1. For that matter, the statistical significance of the improvement in Table 4 is not large, but we choose to be guided by physical reasoning and believe the result. We would bet on the next sample.



maximum cannot be unambiguously identified; then the storm is presumed to have lost its identity. This did not happen in the 1975 sample, the predicted storms being more persistent than the observed ones, especially after land-fall. In all cases the predicted storm position, however obtained, was adjusted by a vector correction appropriate to the vector discrepancy between the specified initial position and the position which emerged from the analysis and initialization procedure.

It occurred to us that since the predicted position of the stream-function minimum may be strongly affected by truncation error, and since the physical basis of the forecast is conservation of absolute vorticity, the position of the storm should be identified with that of the absolute vorticity maximum at all times. Strictly speaking, the relative vorticity maximum is the relevant entity and the absolute maximum will be found slightly to the north. The strength of the earth-vorticity field, however, is utterly small compared to that of the relative-vorticity field, so that the discrepancy is undoubtedly negligible. Moreover, the latter is not explicitly carried in the forecast. Therefore, we are satisfied with the position of the absolute maximum.

Accordingly, for the rerun predictions, the position errors were recomputed on the basis of the vorticity maximum alone, with results shown in Table 7. The adjustment in this case was based on the small discrepancy between the specified storm position and the initialized vorticity maximum. Surprisingly, the errors are slightly larger, overall and for most storms and ranges. Since the vorticity maximum will lie to the right of the nominal position, we might expect that the left bias in the original rerun forecasts would be reduced. The mean algebraic errors of the two sets of rerun forecasts can be compared from the data in Table 8. We find that indeed the left bias is reduced in the first 24-hour period, overall and for five of the seven storms. For the second period, however, the overall left bias is increased, a result due to Eloise and Gladys. The slow bias in speeds, moreover, is slightly increased.

We believe that these curious results were produced by cancellation of errors in the rerun forecasts based on the nominal position, and that the



TABLE 7. Mean position errors (nautical miles)  
for SANBAR reruns based on vorticity maximum  
alone.

	<u>00 hr</u>	<u>12 hr</u>	<u>24 hr</u>	<u>36 hr</u>	<u>48 hr</u>	<u>72 hr</u>
Amy	0 (7)	65 (6)	108 (5)	154 (5)	245 (5)	422 (3)
Blanche	0 (4)	31 (3)	86 (2)	122 (1)	—	—
Caroline	0 (5)	24 (4)	39 (3)	65 (2)	198 (1)	—
Doris	0 (10)	43 (9)	78 (8)	117 (7)	174 (6)	305 (4)
Eloise	0 (15)	42 (14)	73 (13)	109 (12)	185 (11)	320 (9)
Faye	0 (14)	64 (13)	141 (11)	182 (9)	202 (7)	421 (5)
Gladys	0 (17)	56 (17)	125 (16)	203 (15)	296 (14)	437 (12)
Hallie	0 (2)	100 (1)	—	—	—	—
Mean	0 (74)	51 (67)	103 (58)	154 (51)	229 (44)	385 (33)
Change from original reruns	0	+1	+4	+2	+5	+9

( ) Number in sample

TABLE. 8. Mean algebraic errors of original rerun, forecasts and of reruns based on vorticity maximum alone.

SPEED ERRORS (nm)				DIRECTION ERRORS (nm)			
	Reruns-Orig		Reruns-Vort. Max.	Reruns-Orig		Reruns-Vort. Max.	
	00-24hr	24-48hr	00-24hr	24-48hr	00-24hr	24-48hr	
Storm							
Amy	-5 (5)	-67 (5)	-10 (5)	18 (5)	54 (5)	34 (5)	77 (5)
Blanche	36 (2)	—	-36 (2)	95 (2)	—	74 (2)	—
Caroline	0 (3)	72 (1)	0 (3)	-26 (3)	-139 (1)	-12 (3)	-108 (1)
Doris	-34 (8)	-48 (6)	-34 (8)	-10 (8)	20 (6)	0 (8)	21 (6)
Eloise	-5 (13)	-14 (11)	-12 (13)	-5 (13)	-59 (11)	-12 (13)	-69 (11)
Faye	-74 (11)	-62 (7)	-89 (11)	-44 (11)	-62 (7)	-36 (11)	-53 (7)
Gladys	-82 (16)	-142 (14)	-84 (16)	-13 (16)	-6 (16)	2 (16)	-18 (14)
Mean	-43 (58)	-72 (44)	-50 (58)	-11 (58)	-21 (44)	-4 (58)	-22 (44)

( ) Number in sample

biases in these forecasts would have been larger, and the position errors also larger, than in forecasts based on the vorticity maximum alone, had not this cancellation occurred. How this comes about is shown in Fig. 3. The initial correction for the nominal-position forecasts is toward the northeast, on the average, because the average storm is embedded in a southeasterly large-scale flow and the initialized stream-function minimum is too far to the southwest. When this minimum disappears in the course of these forecasts, as more than half did by 48 hours, the position (now based solely on the vorticity maximum) receives an undeserved boost toward the northeast, tending to reduce the average bias in the forecast position. The vorticity-maximum forecasts do not receive this benefit because the initial discrepancy, and thus the correction, is small. When the differences in the corrections for the nominal-position and vorticity-maximum forecasts (seen in Fig. 3) are compared with the differences shown in Table 7, it appears that the success of the nominal-position forecasts was probably a happy procedural accident.

Needless to say, this result could not be expected in a sample of forecasts containing relatively fewer recurving, accelerating tracks; and we recommend use of the vorticity maximum alone, because it makes better physical sense. Finally, however, the entire matter is not very important; the ten-mile reduction of error, which is the most that could be expected, would have little impact on the state of the art. The major areas of prospective improvement lie elsewhere.

#### SANBAR ANALYSIS IN OCEANIC REGIONS

Away from regions of adequate rawinsonde coverage, the analysis of the initial large-scale field of motion is not only difficult, but also crucially important for most tropical-storm forecasts. In the SANBAR grid area an array of 44 "bogus points" was established (Fig. 4) by subjective appraisal of need. Estimates of the mean tropospheric wind at these points, however obtained, were regarded as having the same statistical properties as rawinsonde wind observations, and were therefore used in the construction of

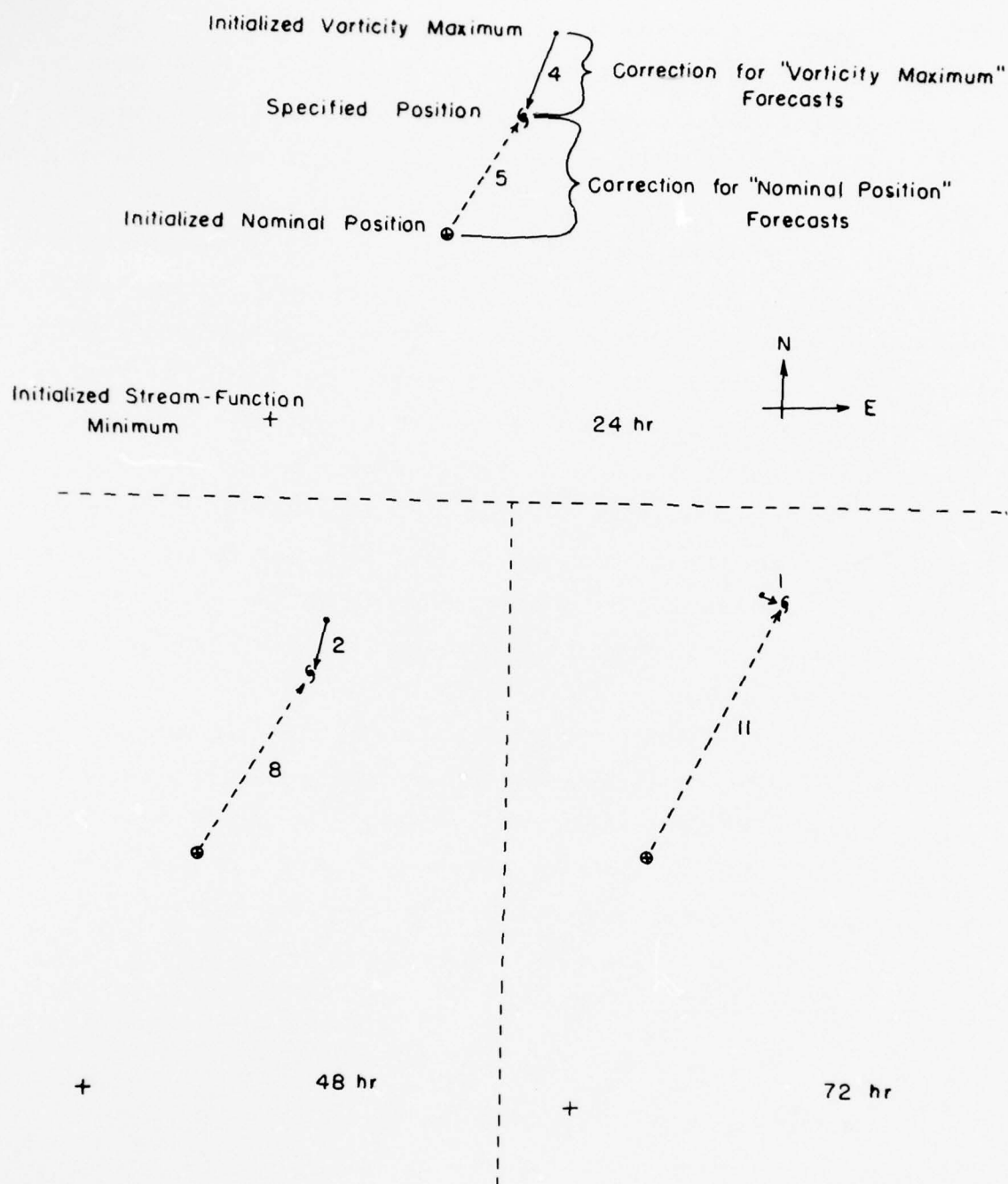


Figure 3. Sketches of correction for "nominal position" forecasts and for "vorticity maximum" forecasts, with actual values of mean discrepancies given in nautical miles. See text.

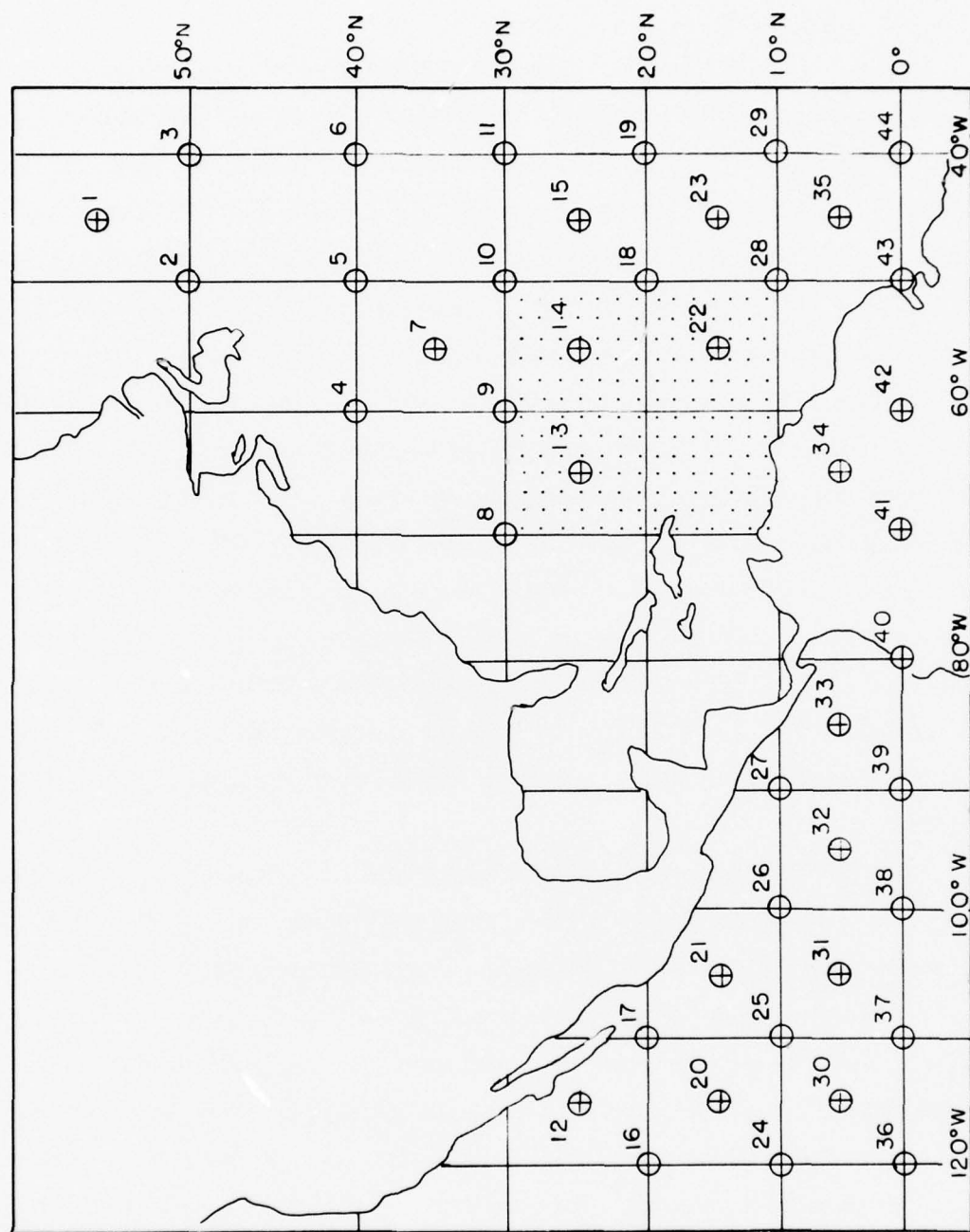


Figure 4. Map of SANBAR grid with bogus points and sample of computational grid



regression equations for performing the analysis at the relevant points of the SANBAR computational grid.

Initially ( in 1968), the bogus-point values were obtained subjectively by a judicious blend of the current operational surface and 200-mb analyses prepared manually at NHC and the 500-mb analysis (at higher latitudes) prepared by NMC, occasionally seasoned with winds observed by reconnaissance aircraft. These information sources, save the last, were generally 12 hours old at the time the bogus-point estimates were made. The procedure, moreover, was awkward and time-consuming.

In time, the process of analysis of the flow pattern at low levels (ATOLL) and near 200-mb was automated (Wise and Simpson, 1971), at NHC; the automation of bogus-point estimation was soon to follow ( Pike, 1972). Further and most importantly, a new data source became available: estimates of wind based on cloud-motion vectors obtained from successive views from geosynchronous satellites. The cloud elements were morphologically characterized as "low", "middle", or "high". The first and last were added to the data base for the ATOLL and 200-mb analyses, respectively. The middle-cloud motions, which were rarely obtained, were not used systematically at NHC.

Pike (1975) derived regression equations for estimating the tropospheric mean wind, required by SANBAR, using wind observations at 850 mb and at 200mb as predictors. In the small dependent data sample, rawinsonde observations at these levels were presumed to simulate winds derived from ATOLL and 200-mb analyses in actual application. Adams and Sanders(1975) established comparable regression equations from a very large sample of data, from the Pacific as well as the Atlantic sector, stratified by geographical area and by season. Their results, for the area corresponding most closely to Pike's are shown in Table 9, along with his earlier results. As can be seen, they found little advantage in stratifying by season.

In view of the difference between these definitive equations and Pike's , and in view of lack of knowledge of the adequacy of the automated ATOLL

TABLE 9. Regression equations for zonal and meridional components (knots) of mean tropospheric wind, based on rawinsonde observations at 850 mb and 200 mb.

Pike (June - November)

$$\frac{\Delta}{u}_{1000-100} = -0.512 + 0.561 u_{850} + 0.399 u_{200}$$

$$\frac{\Delta}{v}_{1000-100} = 0.574 + 0.269 v_{850} + 0.265 v_{200}$$

Adams and Sanders (June-October)

$$\frac{\Delta}{u}_{1000-100} = 0.394 + 0.530 u_{850} + 0.374 u_{250}$$

$$\frac{\Delta}{v}_{1000-100} = -0.513 + 0.450 v_{850} + 0.327 v_{250}$$

Adams and Sanders (June-August)

$$\frac{\Delta}{u}_{1000-100} = 0.268 + 0.538 u_{850} + 0.355 u_{250}$$

$$\frac{\Delta}{v}_{1000-100} = -0.515 + 0.437 v_{850} + 0.322 v_{250}$$

Adams and Sanders (September-October)

$$\frac{\Delta}{u}_{1000-100} = 0.581 + 0.521 u_{850} + 0.386 u_{250}$$

$$\frac{\Delta}{v}_{1000-100} = -0.451 + 0.467 v_{850} + 0.332 v_{250}$$

and 200-mb analyses,<sup>1</sup> we decided to reanalyze the oceanic data base for a selection of cases from the 1975 season. The original intent was to obtain revised values at the bogus points at these two levels, and to use Adams's and Sanders's equations to estimate the tropospheric mean. The list of cases is given in Table 10. We initially selected 18 bad forecasts and 18 good ones from the operational sample, expecting that the bad ones would show improvement and the good ones deterioration; and hoping that the improvement would exceed the deterioration. The first result would likely ensue even if our alterations had no real merit, while the second would assure that we had in fact done something helpful. In the event, one of the good forecasts could not be rerun.

Upon our realization, however, that the ATOLL and 200-mb analyses are now performed exactly on the SANBAR computational grid, the use of bogus points seemed to make little sense<sup>2</sup>. Unless the NHC analysis algorithms were egregiously bad, more useful information could be brought to bear by applying the regression equations directly to the analyzed data at the SANBAR computational grid. Accordingly, we are carrying out the revised forecasts on the basis of a revised analysis technique which makes no reference to the bogus points and uses data directly from the ATOLL and 200-mb analyses in regions sufficiently removed from rawinsonde observations. The results of these revisions will be discussed in a later scientific report.

---

1. We feel that the distinction between Pike's use of 200-mb winds and Adams's and Sanders's use of 250 mb is of little consequence. The NHC 200-mb analysis, based primarily on aircraft observations over the oceans probably more nearly represents 250 mb anyway.

2. Except poleward of  $45^{\circ}\text{N}$ , the northern limit of the ATOLL and 200-mb analyses.

TABLE 10. List of cases for revised forecasts.

## STORM PARAMETERS\*

Storm	Date mo/day	Initial Time (GMT)	Max Wind (kts)	Eye Diam. (nm)	Oper. Dir/Spd (°/kts)	Best Track Dir/Spd (°/kts)	Remarks
Amy	06/30	1200	60	20	030/06	035/03	good at 48 and 72 hrs.
	07/01	0000	60	20	090/03	090/04	bad at 72 hrs.
	07/02	1200	60	20	080/05	090/06	bad at 24 hrs.
	07/03	0000	45	30	065/10	070/11	bad at 24 hrs.
Caroline	08/29	1200	55	20	284/08	270/06	good at 48 hrs.
	08/30	1200	70	10	280/07	295/05	good at 24 hrs.
Doris	08/30	1200	50	20	090/03	090/05	good at 72 hrs.
	08/31	1200	65	20	115/08	095/05	bad at 48 and 72 hrs.
	09/01	1200	75	20	075/01	020/06	bad at 48 hrs.
Eloise	09/16	0000	35	35	285/07	**	good at 24 and 48 hrs.
	09/16	1200	35	25	275/11	280/08	good at 48 and 72 hrs.
	09/18	0000	65	25	275/10	275/11	good at 48 and 72 hrs.
Faye	09/22	0000	45	30	275/05	275/07	good at 24 hrs.
	09/25	1200	40	30	310/09	315/08	bad at 48 and 72 hrs.
	09/26	0000	60	30	315/11	330/11	bad at 24 and 72 hrs.
	09/26	1200	65	30	325/18	330/19	good at 24 hrs.
Gladys	09/26	1200	65	30	280/12	275/16	good at 72 hrs.
	09/28	1200	75	30	270/10	295/08	bad at 24 hrs.
	09/29	0000	65	30	300/10	315/13	good at 72 hrs.
	09/30	0000	90	20	295/14	295/14	good at 48 hrs; bad at 72 hrs.
	09/30	1200	90	15	290/13	295/13	good at 24 hrs; bad at 48 & 72 hrs.
	10/01	0000	90	20	270/13	295/13	bad at 24 and 48 hrs.
	10/01	1200	90	15	340/12	330/12	bad at 48 hrs.
	10/02	0000	120	12	334/20	360/17	bad at 24 hrs.

\* Radius of influence assumed 300nm in all cases except Gladys, 09/28, 1200GMT, and Gladys, 09/29, 0000GMT, for which radius assumed 200nm.

\*\* Best track vector unobtainable since 6-hr displacement prior to initial time unknown.



## DIAGNOSIS OF ERROR IN SOME 1975 FORECASTS

Prior to analyzing the revised forecasts described above, we undertook a study of the particularly poor operational forecasts listed in Table 10, with the aim of determining the causes of large forecast error and of estimating what improvement might be expected from a better analysis of the initial large-scale flow pattern. We found a variety of circumstances leading to especially bad forecasts, the major ones occurring in the case histories to be discussed below.

### Amy, July 3, 0000GMT

This storm (see Fig. 1) originated as a depression over the Gulf Stream east of Florida and reached tropical storm strength east of Cape Hatteras on July 1. It reached hurricane strength only briefly, if at all, before accelerating northeastward, losing its identity east of Newfoundland on the 4th. Amy's main effect was to harass yachts competing in the eastbound transatlantic race. And to damage yachts cruising between Bermuda and the United States, taken unaware by this early-season storm of semi-tropical character. (Hebert, 1976). [According to Van Gemert (1977), winds about 40nm north of the center late on the 3rd were between 50 and 60 knots, with seas to 25 or 30 feet. Conditions were evidently somewhat worse closer to the storm center].

The details of the predicted and observed tracks appear in Fig. 5. The operational track direction and speed at the initial time was toward  $065^{\circ}$  at 10 knots. The storm was predicted to move in approximately this direction and to accelerate only slightly; 14 knots in the first 24 hours and 17 knots in the second.<sup>1</sup> In the event, the storm curved slightly to the left and accelerated dramatically to 24 knots 12 to 24 hours after initial time. The result was a large 205-nm error in the forecast position at 24 hours range, with

---

1. The jog of the forecast track to the right between 36 and 48 hours is an artificial result of the loss of stream-function minimum, as discussed earlier.



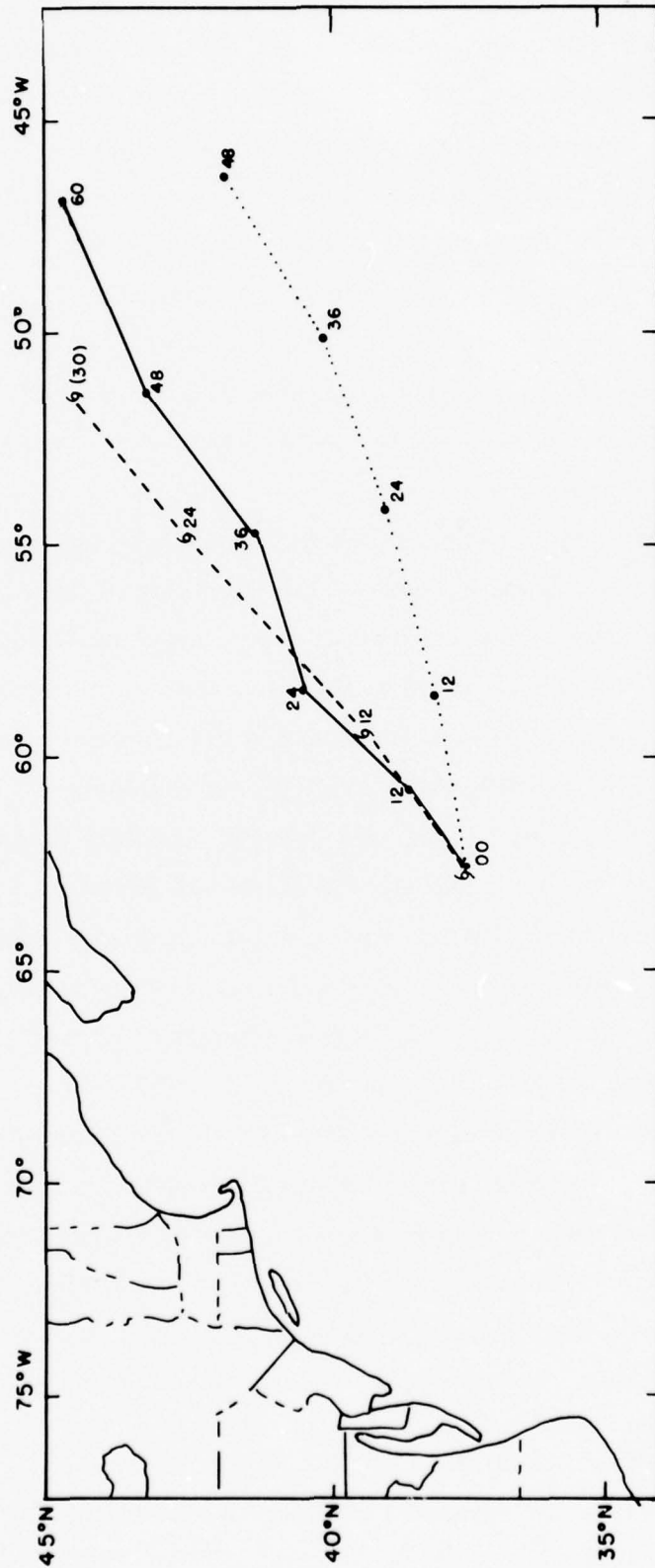


Figure 5. Tracks of Amy, July 3, 0000GMT. Dashed lines indicate observed tracks; solid lines, operational track; and dotted lines, best-track rerun. Dots show forecast positions, labelled with the appropriate number of hours after initial time. Corresponding observed positions are shown by hurricane symbols with open centers, indicating tropical storm strength.

commensurately large errors at later times had we not received the blessing of dissolution of the actual storm. The best-track position and track velocity were close to the operational values and would have led to no great improvement in this forecast, but we provided an erroneous velocity toward  $075^{\circ}$  at 18 knots for the rerun, yielding the modified track shown. The storm failed to accelerate through the first 48 hours of the forecast. (This case, of course, was not included in the sample of 74 discussed in earlier sections.) The failure of either the operational or the spurious rerun forecasts to show early acceleration led us to believe that the initial large-scale analysis may have been seriously in error.

This flow pattern, from the operational SANBAR run, appears in Fig. 6. Filtering of the storm leaves a large-scale flow toward the east-northeast at about 10 knots over the initial position of Amy, while large-scale confluence produces a speed of about 20 knots at the 24-hour forecast position.<sup>1</sup> Thus, the first 24-hours of the forecast track was a direct consequence of the initial analysis; its temporal evolution was of little consequence.

The data bases for the ATOLL and 200-mb analyses (supplemented by some data evidently not available in real time) are shown in Fig. 7. In the crucial area, say, bounded by the center of storm, bogus points 7 and 5, Newfoundland and Nova Scotia, there are few observations to guide the ATOLL analysis. At 200mb, a number of reports of strong southwesterly winds lie in this area, but not at bogus points 5 and 7.

The strong wind observed by the ship at  $37^{\circ}\text{N } 59^{\circ}\text{W}$  and the strong south-southwesterlies at 200 mb derived from satellite observations near  $37^{\circ}\text{N } 57^{\circ}\text{W}$  as well as the estimated value at bogus point 4 would have been ignored since they lie within the maximum influence distance of the storm. It is clear from the storm parameters (Table 10) that the synthetic analysis at  $37^{\circ}\text{N } 59^{\circ}\text{W}$  would yield a much weaker mean wind than any reasonable re-

---

1. A useful rule of thumb is that the wind speed in knots is 10 times the number of stream-function channels contained in a distance of 300 nm (5 degrees of latitude).

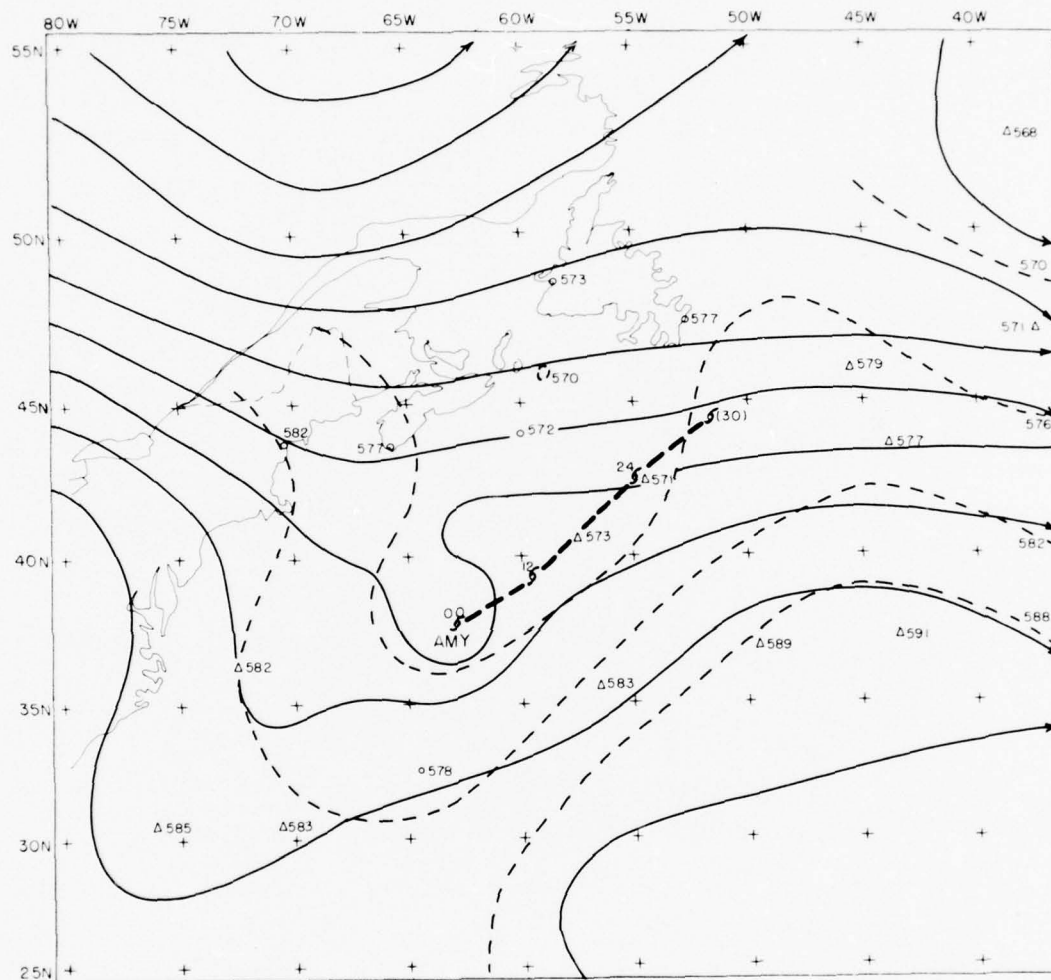


Figure 6. Initial analysis of large scale flow pattern, July 3, 0000GMT. Solid lines are isoplths of stream function, at intervals of  $300 \times 10^4 \text{ m}^2 \text{ s}^{-1}$  from the operational SANBAR analysis. Dashed lines are subjectively analyzed 500-mb contours at intervals of 6 dm. Triangles indicate 500-mb heights obtained from satellite data; circles, from rawinsonde observations.

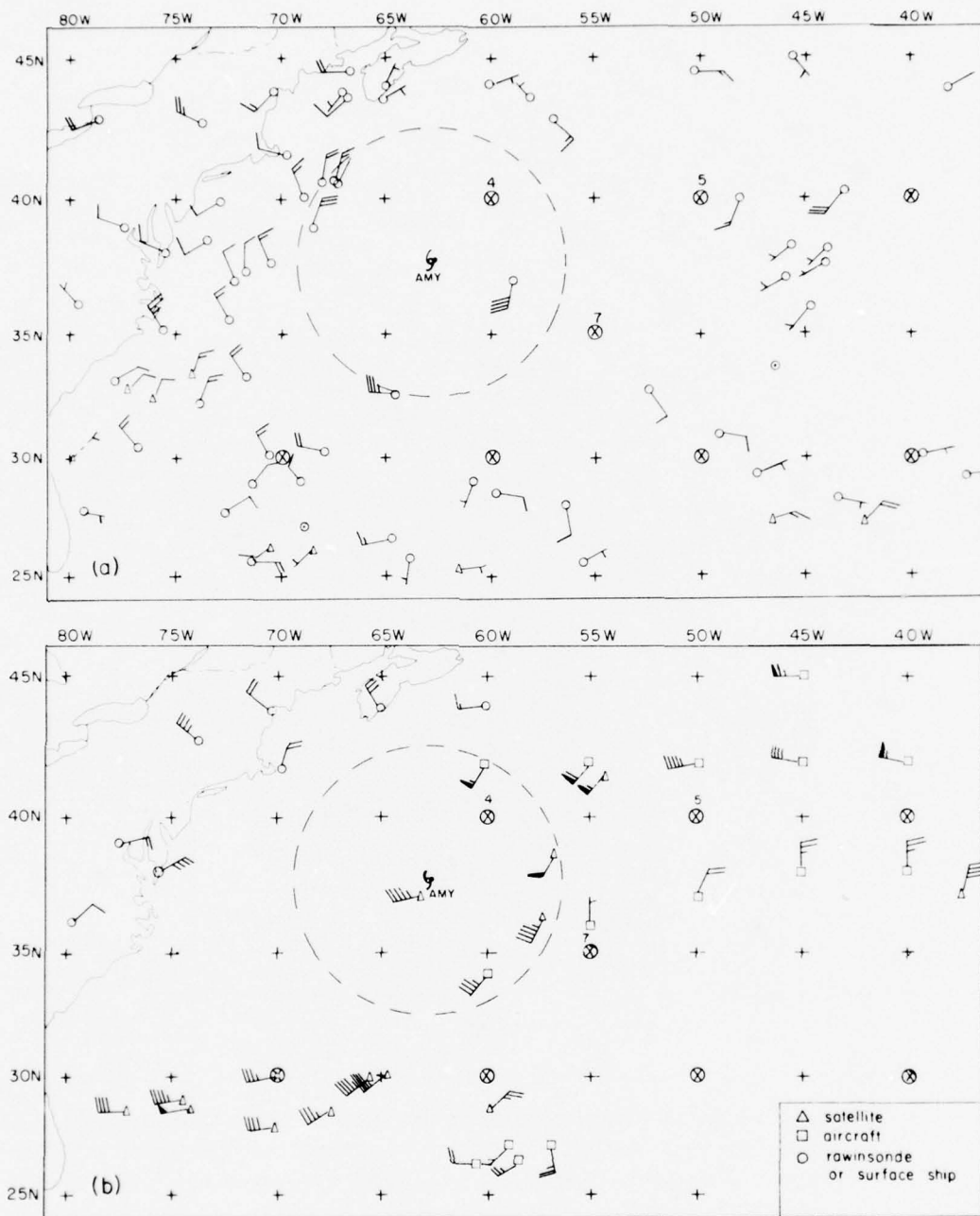


Figure 7. Data bases for oceanic analysis, July 3, 0000GMT  
a) ATOLL; b) 200-mb. Positions of bogus points are shown by circled x's. Radius of influence is shown by the dashed circle. Dashed arrows indicate data not in NHC collection.

gression estimate based on direct analysis of the observed data. Inspection of Fig. 5 confirms this expectation. At  $42^{\circ}\text{N } 55^{\circ}\text{W}$  a combination of the wind observed by aircraft and an estimate of  $140^{\circ}$  at 15 knots estimated from the ATOLL data would yield, upon application of Adams's and Sanders's June-October regression equations, a tropospheric mean wind of  $207^{\circ}$  at 22 knots. An analysis based only on rawinsonde and bogus observations would not detect this wind; and Fig. 5 shows a direction of about  $260^{\circ}$  at this point<sup>1</sup>. In all, the initial large-scale analysis appears to be seriously in error, to the considerable detriment of the forecast.

In this case, it further appears that constant-pressure height data, studiously avoided in the tropically-oriented SANBAR system,<sup>2</sup> might have been helpful. Fig. 8 contains the heights at the 500-mb level, which yields a geostrophic wind in close approximation to the tropospheric mean wind. In addition to values at the rawinsonde stations, a number of estimates were made by adding a 1000-mb height derived from the sea-level pressure analysis to the thickness of the layer from 1000mb to 500mb derived from SIRS temperature soundings from the NOAA-5 polar orbiter. A subjective analysis of the 500-mb contours, based on these data, appears in Fig. 8(a) (Though the satellite-derived heights are clearly poorer than the rawinsonde observations, the time series of rawinsonde data at Bermuda, near  $32^{\circ}\text{N } 65^{\circ}\text{W}$ , suggests that the observed height is erroneously low at this time and that the satellite data are essentially correct.) The subjective analysis yields geostrophic winds which are in accord with our foregoing estimates based on observed wind data. A comparison of the wind fields derived from the subjectively

---

1. The large discrepancy between the stream flow and the observed wind at Shelburne, Nova Scotia (near  $44^{\circ}\text{N } 65^{\circ}\text{W}$ ) is due to the omission of this recently-installed station from the list used in the SANBAR regression equations. This list and the dependent equations should be updated immediately.

2. This is a slight overstatement, since the ATOLL and 200-mb analyses use NMC grid-point wind values as a first guess, and these have been derived in part from rawinsonde and satellite heights.





smoothed SANBAR initial analysis and from the 500-mb geostrophic analysis appear in Fig. 8.

We observe, incidentally, from the ATOLL data that the storm influenced a region with a radius of about 500 nm rather than the nominal 300-nm value used in the SANBAR calculation. This problem, however, is interrelated with the yet unresolved problem of how to deal effectively with data within the influence region of the storm, as discussed by Sanders *et al.* (1975). These important problems are not addressed in our present work.

We conclude that the poor forecast of the track of Amy was due in this instance to faulty initial analysis of the large-scale flow surrounding the storm.

#### Faye, September 26, 0000GMT

This storm was first detected as a typical westward-moving tropical depression in the central Atlantic on September 18. The track in Fig. 1 shows that Faye barely reached hurricane strength by the initial time of this forecast, after a long gestation period. She had begun recurvature on the 24th, moving slowly and somewhat erratically. With acceleration and recurvature into the middle-latitude westerlies far from land, Faye represented only a threat to shipping. This threat may have been considerable, however, since her abrupt eastward acceleration on the 28th brought her path to speeds which only the fastest and strongest ships could out-manuever.

The SANBAR and actual tracks are shown in detail in Fig. 9, for the prediction starting at 0000GMT on the 26th. Position errors for both the operational and the best-track rerun forecasts are given in Table 11.

TABLE 11. Position errors (nautical miles) in SANBAR forecasts for Faye, September 26, 0000GMT.

<u>Forecast</u>	<u>Initial track</u>		<u>0 hrs</u>	<u>24 hrs</u>	<u>48 hrs</u>	<u>72 hrs</u>
	<u>Dir. (°)</u>	<u>and Spd(kts)</u>				
Operational	315	-11	21	212	345	961
Best track rerun	330	-11	0	183	253	772
Change from operational			-21	-29	-92	-189

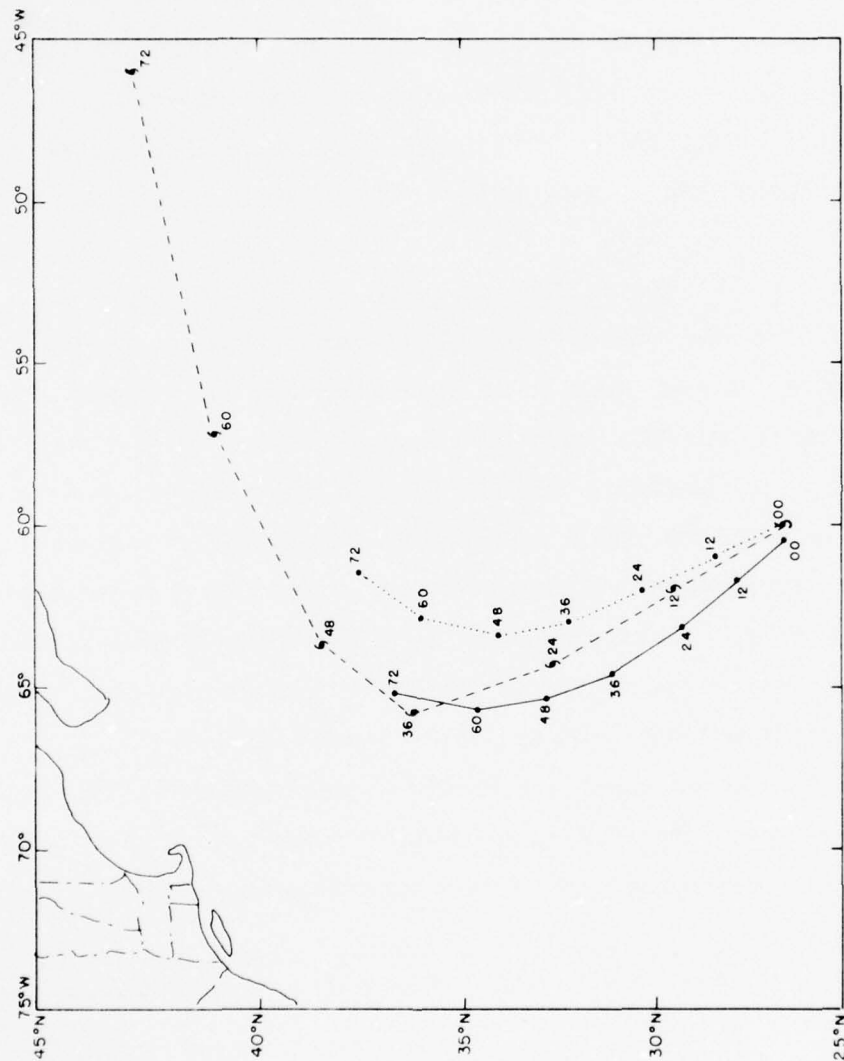


Figure 9. Tracks of Faye, September 26, 0000GMT. Hurricane symbols with closed centers indicate storm of hurricane strength. Other notation the same as Figure 5.

The best-track information reduced the position errors considerably, with the improvement increasing monotonically to 72 hours. Reference to Fig. 9, however, shows that the 24-hour benefit was due solely to the improved track direction in the best-track forecast, and that the reduced errors at later times were attributable mainly to the preliminary recurvature in the rerun forecast. Speed was a major problem in both cases: both the immediate jump from the initial 11 knots to an actual 17 knots, and the observed mighty increase in speed from 48 to 72 hours. Thus, we believe that the large-scale flow was both incorrectly analyzed initially and unusually badly predicted.

The initial stream-function pattern appears in Fig. 10, while the data bases for the ATOLL and 200-mb analyses appear in Fig. 11. At bogus points 9, 13, and 14, at Bermuda, and at  $20^{\circ}\text{N } 60^{\circ}\text{W}$  it was possible to compare large-scale winds derived from the stream pattern with winds computed from subjective estimates from the ATOLL and 200-mb data bases. These estimates agreed with operational values at some but not all of these points. In cases of disagreement, an observation was close to the point. It can be seen from the results in Fig. 10 that the directions of the stream-function and estimated winds agree closely except at bogus point 14, where the latter is substantially veered from the former. The estimated speeds, however, are greater without exception, substantially so near and perhaps south of the center. These speeds, in fact, correspond in the mean closely to the average of the actual track speeds six hours prior and 12 hours after the initial time. (A correct initial analysis, after all, should provide a good hindcast as well as a good forecast.) There is some indication of a downstream increase in speed, suggesting acceleration along the track, but not the sudden speedup observed.

The question then arises why the SANBAR predicted speeds in the first 24 hours were so slow. First, winds derived from observations at bogus points 9 and 13 were discarded, since they lie within the outer portions of the 300-nm radius deemed to be influenced by Faye. They were replaced by weaker winds based on the 11-knot initial track speed. It appears, then, that the present SANBAR analysis algorithm loses valuable information in

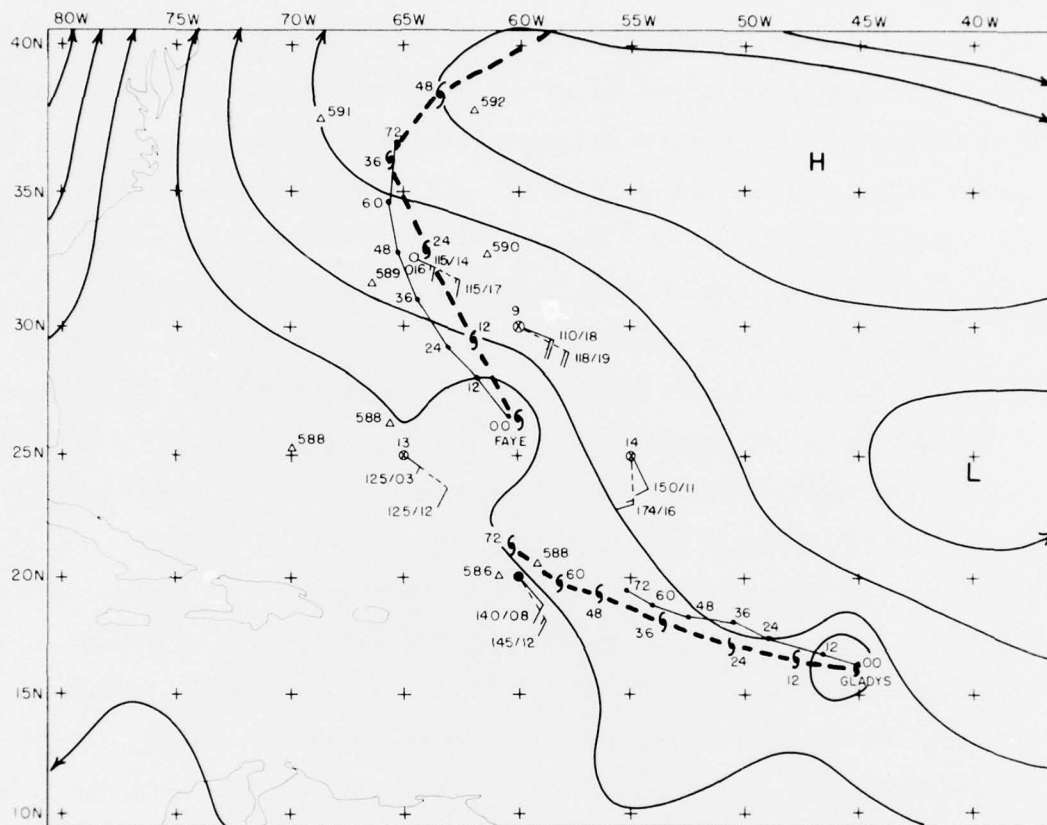


Figure 10. Initial SANBAR operational flow pattern, September 26, 0000GMT. Solid arrows indicate winds derived from stream-function pattern. Dashed arrows indicate winds estimated from ATOLL and 200-mb data bases.



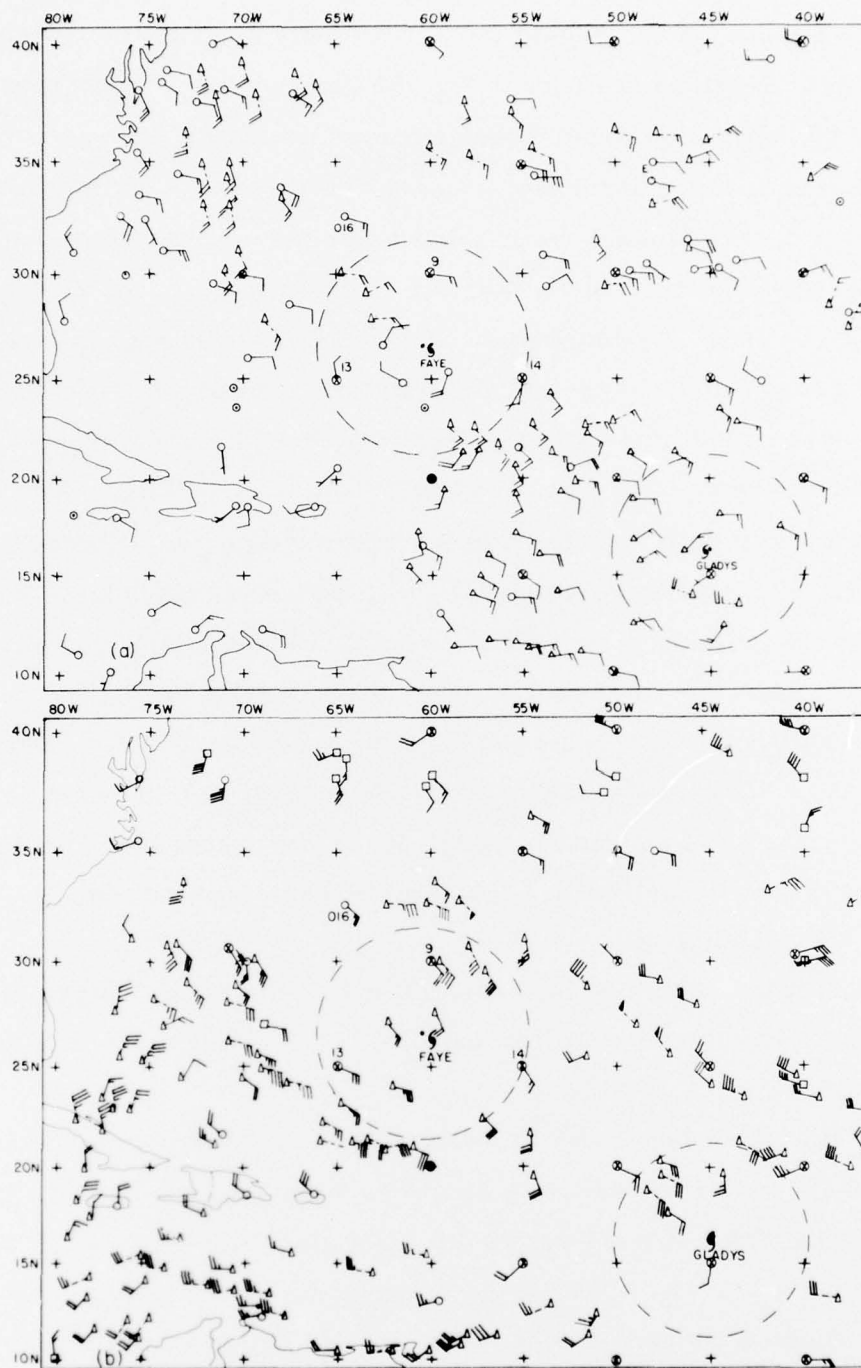


Figure 11. Data bases for oceanic analysis, September 26, 0000GMT: a) ATOLL; b) 200-mb. Notation the same as Figure 7.

the outer portion of the region influenced (only slightly) by the storm.

Second, it can be seen from Fig. 11 that the large-scale flow displayed substantial, well-organized, shear between the lower and upper troposphere in the region surrounding Faye. An equivalent-barotropic effect could easily be added to the SANBAR forecast, but as pointed out by Sanders et al. (1975), it is in general neither substantial nor reliable in the tropical regions in which this model is currently employed. (This effect, if applied in the present instance, would yield a better short-term forecast but a poorer hindcast; on another occasion it might be the other way around.) Fig. 11 also shows that Faye was embedded in a large trough system in the ATOLL layer. This presumably same trough is evident in the 200-mb data, with stronger circulation and substantial southward displacement. There is undoubtedly positive thermal-vorticity advection over Faye, similar to developing extratropical cyclones, however modest the magnitude in this case. A fully baroclinic model would be required to calculate accurately the consequence of this structure. Hovermale's MFM Model (1975) should be helpful in this respect.

Third, as can be seen from Fig. 10, there are no satellite data to the right of the path of the storm. They might have been helpful, as in the case of Amy discussed above.

In summary, there were obvious flaws in the initial analysis, which were damaging to the short-term forecast. Part of the answer remains shrouded in mystery.

The failure of the model to produce the dramatic forward acceleration observed from 48 to 72 hours is another story, only part of which lies in the failure of SANBAR to put Faye in the right place at 48 hours. The matter is elucidated in Fig. 12, in which the large-scale predicted and observed 48-hour stream-function changes are depicted. Since the stream-function field can be specified only as the residual from an arbitrary constant, some assumption must be made to arrive at these fields. We assumed that the stream-function value remained essentially unchanged in the lower right-hand corner of the grid area.

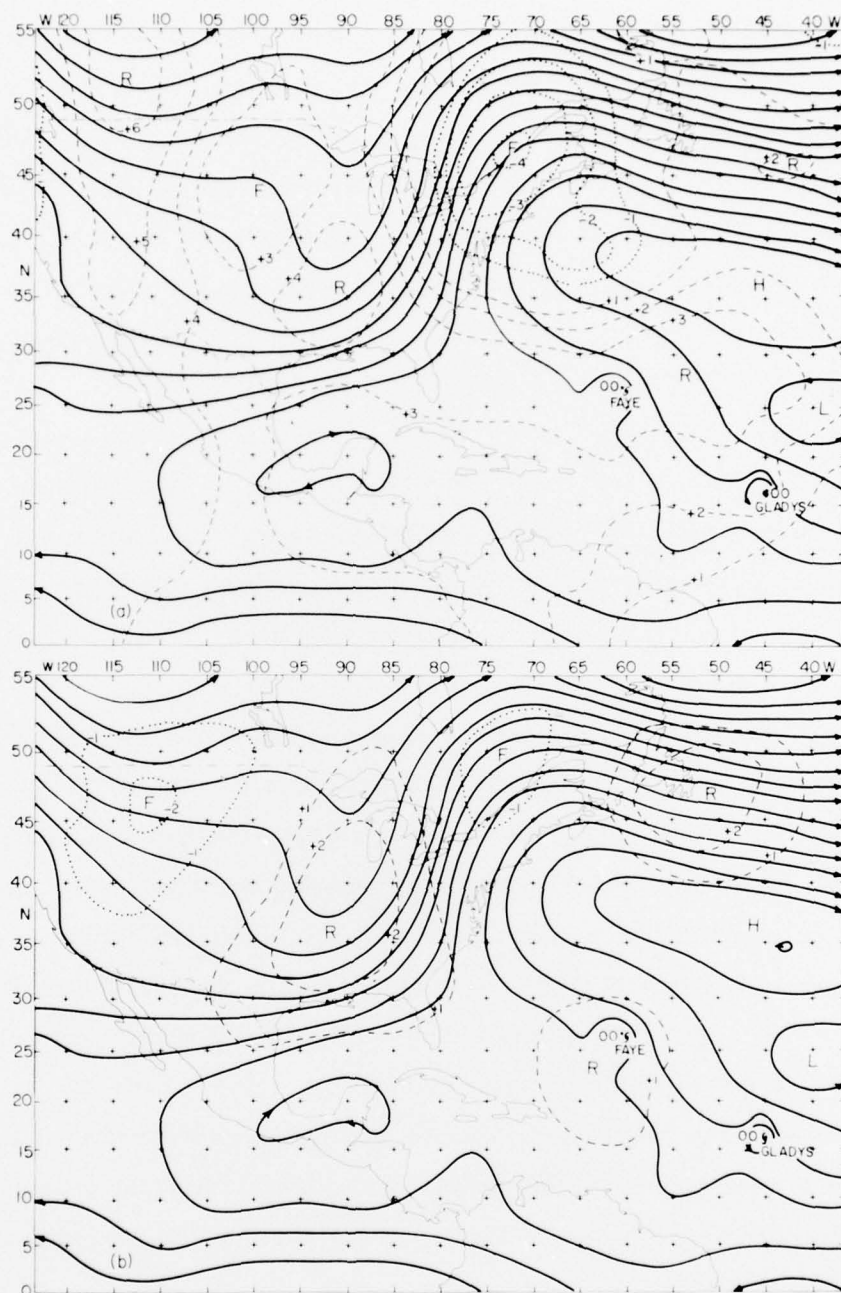


Figure 12. Large scale initial flow pattern (solid lines) and 48-hour stream-function changes: a) observed; b) predicted by SANBAR. Dashed lines indicate stream-function rises; dotted lines, stream-function falls.

We note that the intensity of the forecast changes is not as great as that of the observed ones. This failure is probably typical of any barotropic model. In particular, the predicted gradient of change in the path of Faye was woefully in error. The observed maximum rise along 25°N in the Atlantic was only hinted at in the forecast. There were substantial changes along the boundaries, held approximately constant in the SANBAR forecast, but these were probably not primarily to blame, since the centers of change were well removed from the limits of the forecast grid. Note particularly the prominent center of fall along the St. Lawrence River, due to the advance of the pronounced trough initially in the Mississippi Valley. This prominent change, feebly simulated in the SANBAR forecast, was doubtless responsible, along with the general rise along 25°N, for the observed increase in speed of the storm. The large-scale flow speed in the path of Faye was 25-30 knots and increasing with time.

The large-scale NMC forecasts for approximately this time appear in Fig. 13<sup>1</sup>. It is clear that neither the barotropic nor the six-layer primitive-equation (PE) forecast adequately predicted the substantial changes in the large-scale flow. The PE 72-hour forecast did show the trend, but too little and too late. From this we conclude that, as suggested above, fixed boundary values of stream function were not a major contributor to the SANBAR failure in this case, and that although baroclinic effects were doubtless important they were not adequately represented in the PE forecast.

In summary, the large errors at 48 and 72 hours were due to egregious error in the large-scale SANBAR forecast, principally due to the failure to consider baroclinic effects and only secondarily to the failure to provide for boundary changes.

---

1. Complete sets of NMC forecasts were not available at MIT at this time.



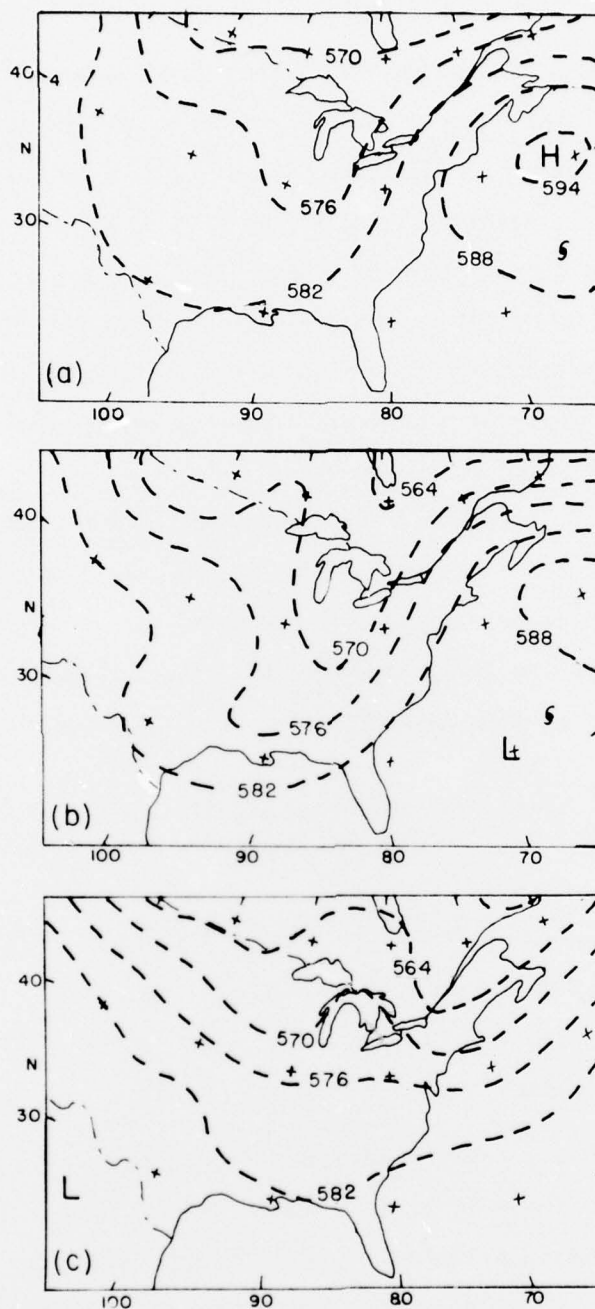


Figure 13. NMC prognostic charts: a) 36-hour barotropic forecast valid at 0000GMT, September 27; b) 24-hour PE forecast valid at 0000GMT, September 27; and c) 72-hour PE forecast valid at 0000GMT, September 29.



Gladys, September 30. 0000 GMT

As shown in Fig. 1, Gladys, like Faye, grew from a tropical depression that doubtless evolved from an easterly wave emerging from Africa (Burpee, 1972). Gladys, however, achieved hurricane strength much more quickly and followed a track somewhat south and west of Faye's, although generally parallel to it. The former storm, in fact, can be seen in Figs. 10-12, at a time when serious SANBAR forecast errors had not yet developed. As in the Faye forecast discussed above, the primary failure is inadequate prediction of northeastward acceleration following recurvature, but the cause in this case is different, as we shall see.

The details of the predicted and observed tracks following the initial time of 0000GMT, September 30 appear in Fig. 14., while the ATOLL and 200-mb data bases appear in Fig. 15. Position errors for the operational and rerun forecasts are given in Table 12. The 24 and 48-hour forecasts in this case are better than average, the latter spectacularly so. There is

TABLE 12. Position errors (nautical miles) in SANBAR forecasts for Gladys, September 30, 0000GMT.

<u>Forecast</u>	<u>Initial track</u>		<u>0 hrs</u>	<u>24hrs</u>	<u>48hrs</u>	<u>72 hrs</u>
	<u>Dir. (<math>^{\circ}</math>)</u>	<u>and Spd(kts)</u>				
Operational	295	14	5	50	15	661
Best track rerun	295	14	0	47	15	675
Change from operational			-5	-3	0	+14

no significant difference between the operational and rerun forecasts, as the position and track velocity were well known in real time. The paucity of initial data, particularly at 200 mb east of Gladys (see Fig. 15), demonstrates that one can be lucky on occasion. The observations in Fig. 15(b), however, are adequate to show the upper-level trough wrapped around the western and southern periphery of the storm, extending thence eastward between latitudes  $15^{\circ}\text{N}$  and  $20^{\circ}\text{N}$ . This feature, undoubtedly the same as the one seen in Fig. 11(b), does not seem in this instance (contrary to the Faye

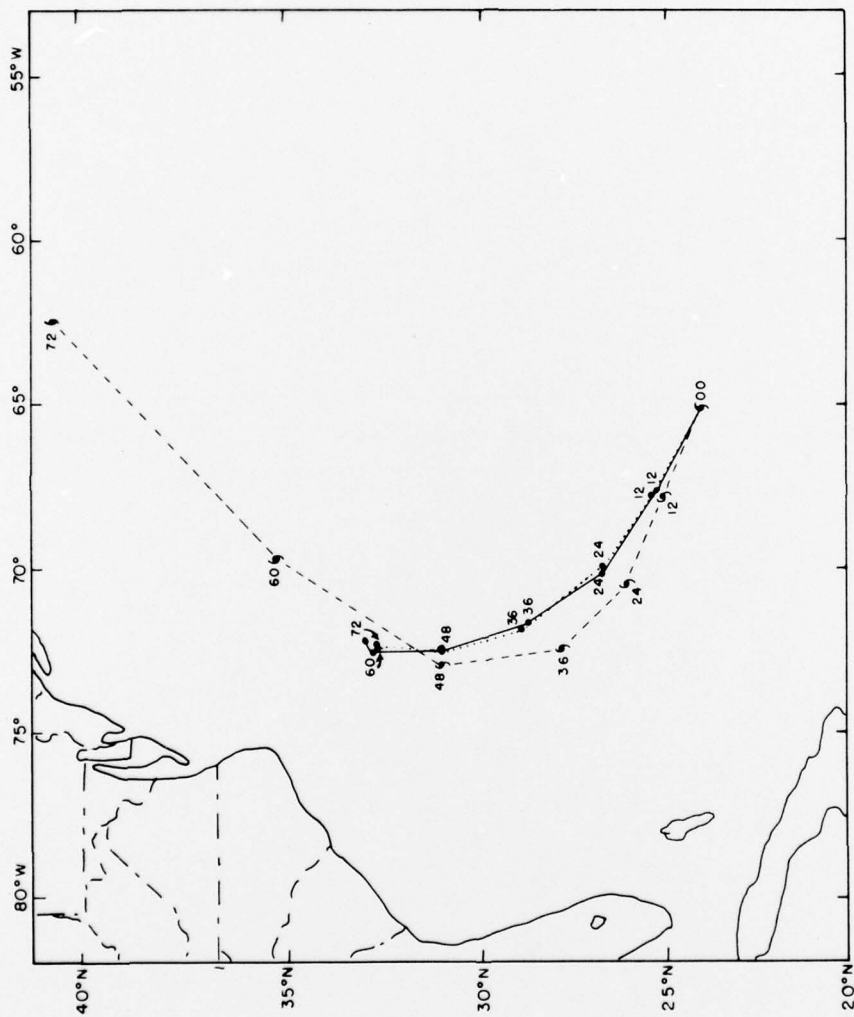


Figure 14. Tracks of Gladys, September 30, 0000GMT.  
Notation the same as Figures 5 and 9.

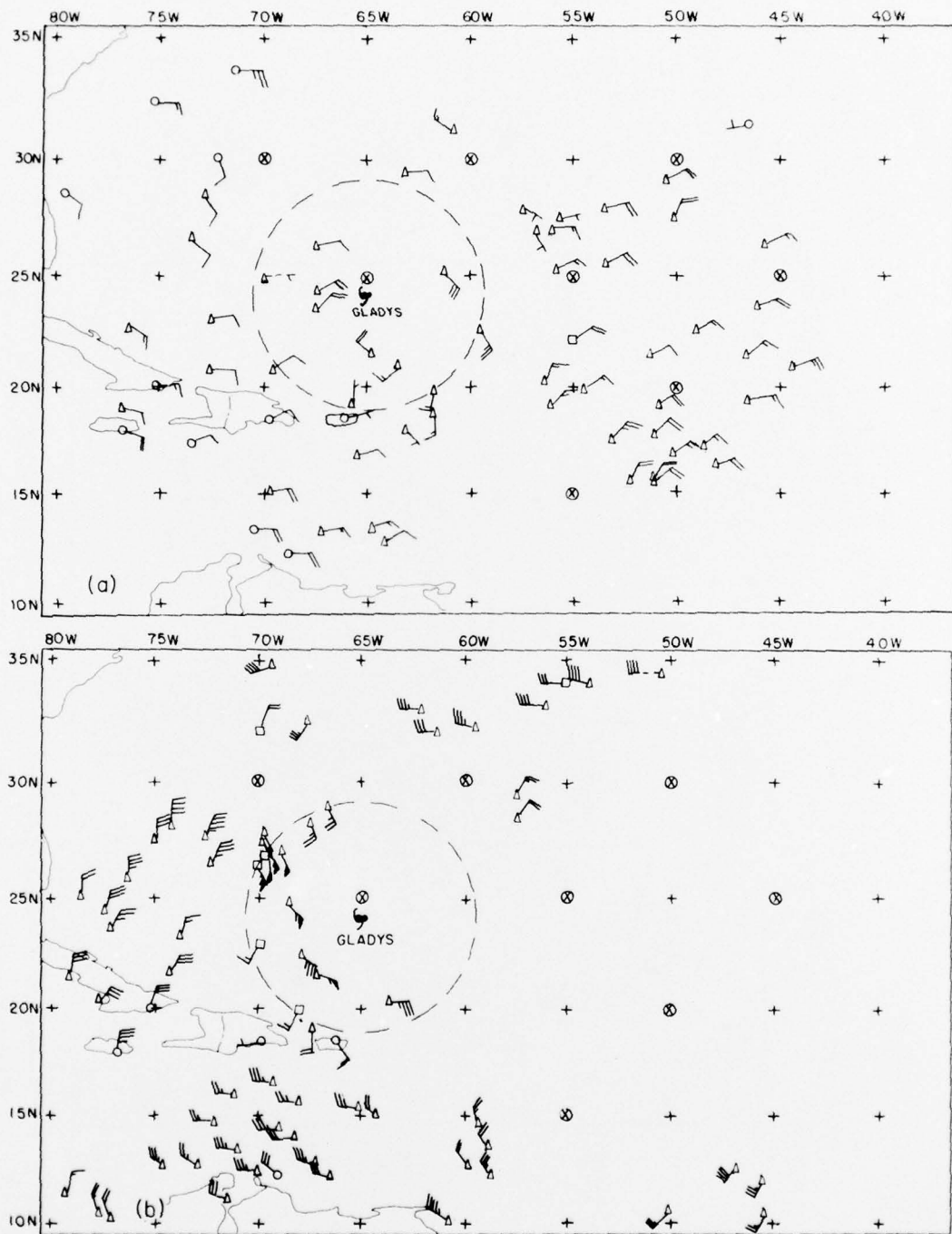


Figure 15. Data bases for oceanic analysis, September 30, 0000GMT: a) ATOLL; b) 200-mb. Notation the same as Figure 7.

case discussed above) to be providing positive vorticity advection over the storm area, in which the flow is nearly symmetric. The difference may be a reflection of Faye's growth vs Gladys's maturity at the time studied.

The large error is in the range of 48 to 72 hours, when Fig. 14 shows that the predicted storm came nearly to a halt while the living Gladys leapt ahead to a speed of 40 knots in the last half of the interval. The flow pattern and 48-hour observed changes shown in Fig. 16(a) display a series of mobile ridges and trough in the westerlies poleward of  $35^{\circ}\text{N}$  with considerable amplitude but little indication of change of intensity. The predicted changes in Fig. 16(b), on the other hand, show little of this mobility but rather a substantial average stream-function rise. The band of maximum rise extending north of the storm path between latitudes  $40^{\circ}\text{N}$  and  $45^{\circ}\text{N}$ , together with the westward displacement of the subtropical anticyclone from an initial position at  $31^{\circ}\text{N } 56^{\circ}\text{W}$  to a position near  $33^{\circ}\text{N } 65^{\circ}\text{W}$  48 hours later explain Faye's subsequent predicted halt<sup>1</sup>. This large-scale anticyclone doubtlessly had settled directly over the storm by 72 hours. The actual storm, on the other hand, was presumably caught up in the strong southwesterly flow between the trough in the Great Lakes region and the downstream ridge over the Canadian Maritime Provinces at 48 hours range.

The failure of the SANBAR forecast in this case has two causes. First, the observed changes were large along the fixed northern boundary while the maximum magnitudes were not far from it. Second, the average flux of earth vorticity into the forecast area appears to be in the anticyclonic sense, primarily because of the influx of low values at the left boundary near latitude  $25^{\circ}\text{N}$  and the efflux of large values at the right boundary near  $40^{\circ}\text{N}$ . While the forecast program is being altered to allow for stream-function changes on the boundary, it might be a good idea to allow for vorticity changes as well. Of course, only the local changes of relative vorticity would count; their importance has not yet been demonstrated but is probably considerable

---

1. Only the initial and 48-hour predicted SANBAR flow patterns are archived by NHC.



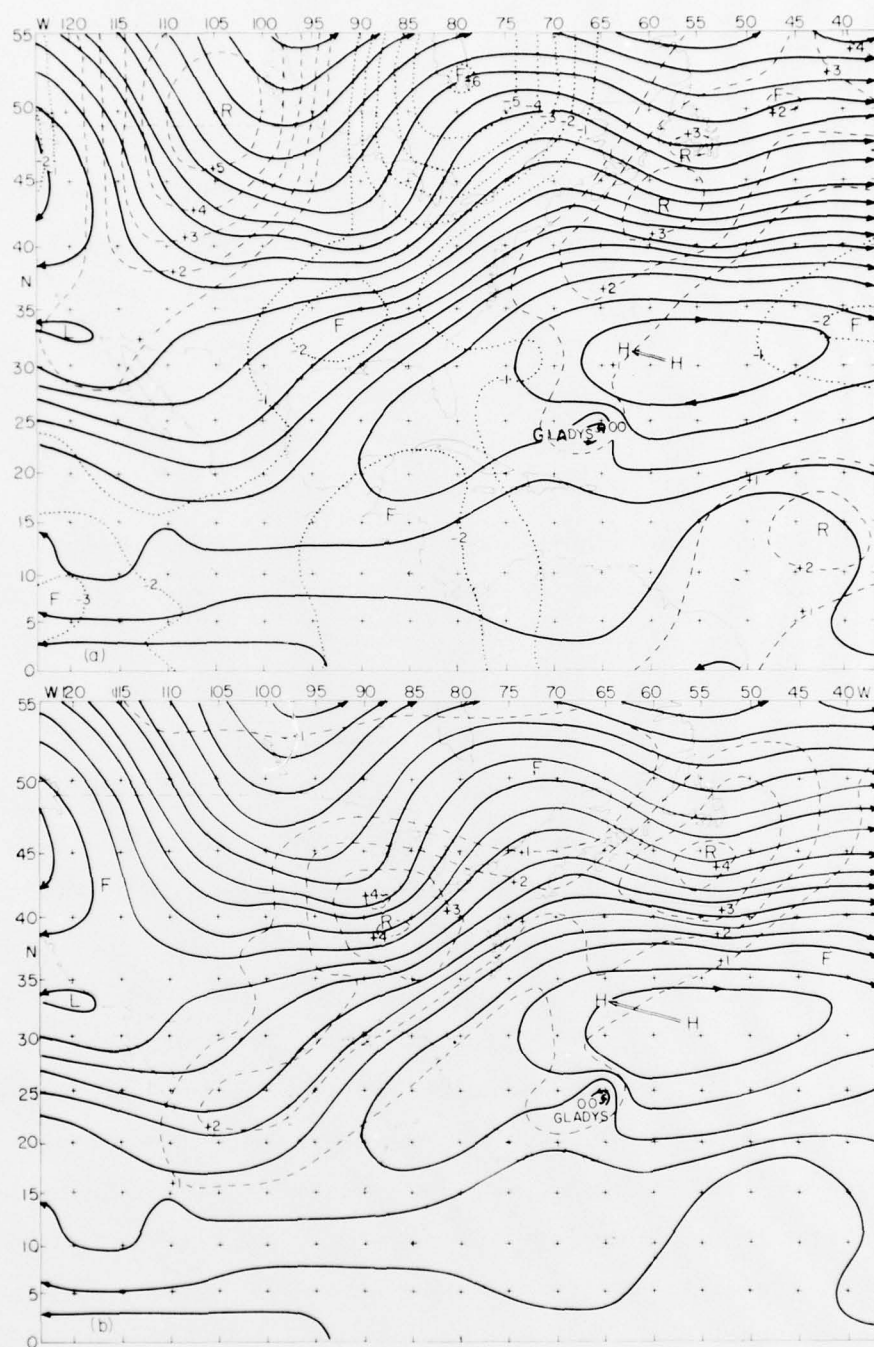


Figure 16. Large scale initial flow pattern and 48-hour stream-function changes: a) observed; b) predicted by SANBAR. Notation the same as Figure 12.



on occasion.

Our diagnosis is supported by the barotropic and PE forecasts shown in Fig. 17. The general trend of events is successfully indicated, especially by the latter, enough so to produce substantial improvement had they been used to predict the storm path but probably not accurately enough to yield a really good 72-hour forecast.

### CONCLUSIONS

Our study of SANBAR forecasts made operationally during the 1975 hurricane season yields the following conclusions and recommendations:

1. A more accurate initial position and track will produce a substantial increase in accuracy of the position forecasts at ranges of 24 hours and probably at 48 hours .
2. The use of satellite-derived heights may provide useful information for prediction of storms initially poleward of, say,  $30^{\circ}\text{N}$ .
3. The current method of analyzing the initial stream-function field in the area influenced by the storm circulation is resulting in loss of useful observational information (mostly satellite-derived wind estimates) in the outer fringes. This method should be altered.
4. The present use of SANBAR bogus points is an unnecessarily complex procedure which is probably losing valuable information contained in increasingly abundant satellite information. The analysis method should be altered, at least over oceanic regions.
5. Fixed values of stream-function and absolute vorticity on the boundaries of the current SANBAR forecast area are producing serious errors in some forecasts beyond 24 hours range. Either the forecast area should be enlarged or predicted values from a hemispheric or global model should be applied to the SANBAR boundaries.
6. Some storm tracks respond to baroclinic effects in the large-scale features of the surrounding region. In some instances the

storm track may be influenced by asymmetric baroclinic effects in the storm structure itself. A baroclinic model, appropriate to the character of the oceanic data base, should be developed.

7. The McIDAS system should be helpful with respect to items 1, 2, 3, and 4.
8. Even when all this is done, we shall still see in part and prophesy in part. But we may hope to see through the glass less darkly.

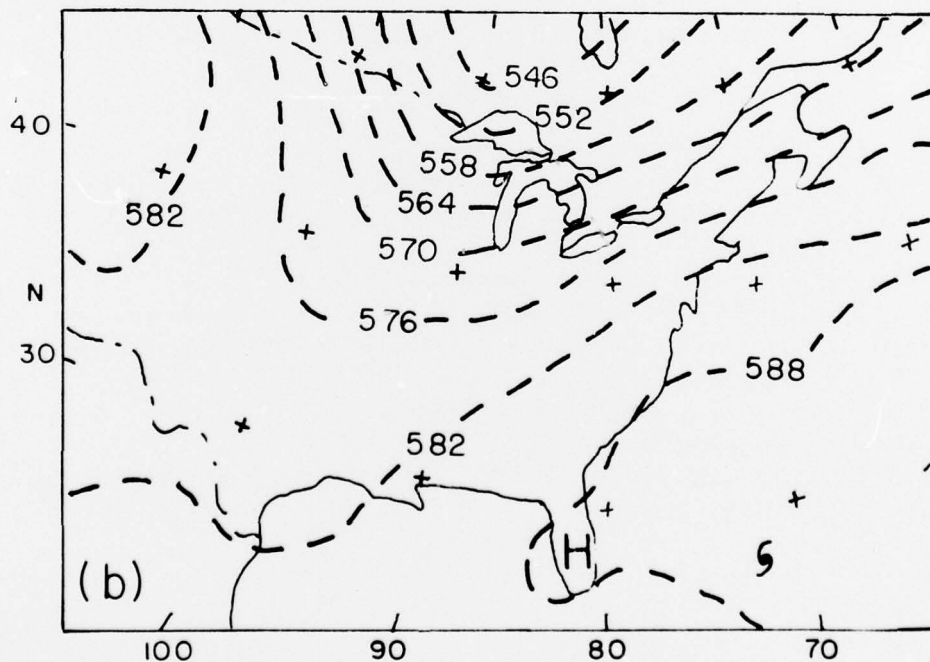
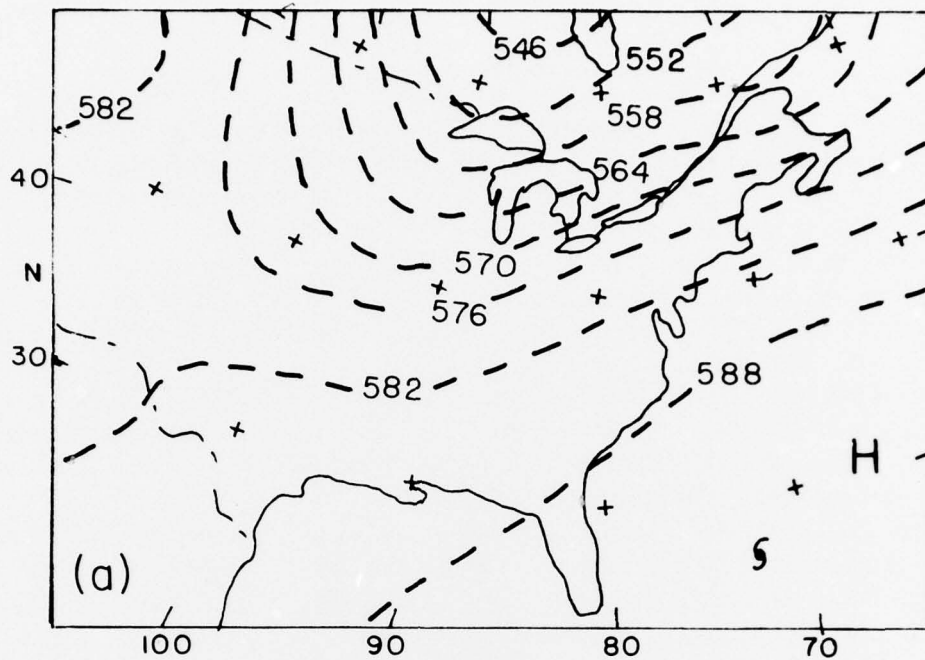


Figure 17. NMC prognostic charts: a) 36-hour barotropic forecast valid at 1200 GMT, October 1; and b) 36-hour PE forecast valid at 1200 GMT, October 1.

## REFERENCES

- Adams, A. L., and F. Sanders, 1975: Application of satellite cloud motion vectors to hurricane track prediction. Massachusetts Institute of Technology. Scientific Report No. 1, AFCRL Contract F19628-75-C-0059. Report number AFCRL-TR-75-0635. 57pp.
- Burpee, R. W., 1972: The origin and structure of easterly waves in the lower troposphere of North Africa. J. Atmos. Sci., 29, 77-90.
- Hebert, P. J., 1976: Atlantic hurricane season of 1975. Mon. Wea. Rev., 104, 453-465.
- Hovermale, J. B., 1975: First season storm movement characteristics of the NMC objective hurricane forecast model. Paper presented at Twelfth Annual NOAA NWS Hurricane Warning Service Evaluation Conference, December, 1975, Coral Gables, Florida.
- Neumann, C. J., and J. R. Hope, 1973: A diagnostic study on the statistical predictability of tropical cyclone motion. J. Appl. Meteor., 12, 62-73.
- , and M. D. Lawrence, 1975: An operational experiment in the statistical-dynamical prediction of tropical cyclone motion. Mon. Wea. Rev., 103, 665-673.
- , J. R. Hope, and B. I. Miller, 1972: A statistical method of combining synoptic and empirical tropical cyclone prediction systems. NOAA Tech. Memo. NWS SR-63.
- Pike, A. C., 1972: Private communication.
- , 1975: Private communication.
- Sanders, F., A. C. Pike, and J. P. Gaertner, 1975: A barotropic model for operational prediction of tracks of tropical storms. J. Appl. Meteor., 14, 265-280.
- Van Gemert, L., 1977: Private communication.
- U. of Wisconsin, 1973: Mean computer interactive data access system (McIDAS). Final Report on Contract NAS 5-21794, 18 August 1973. For Goddard Space Flight Center, Greenbelt, Maryland. Final Report covering period 25 July, 1972 - 24 July, 1973. Science and Engineering Center, Madison.
- Wise, C. W., and R. H. Simpson, 1971: The tropical analysis program on the National Hurricane Center. Weatherwise, 24, 164-173.